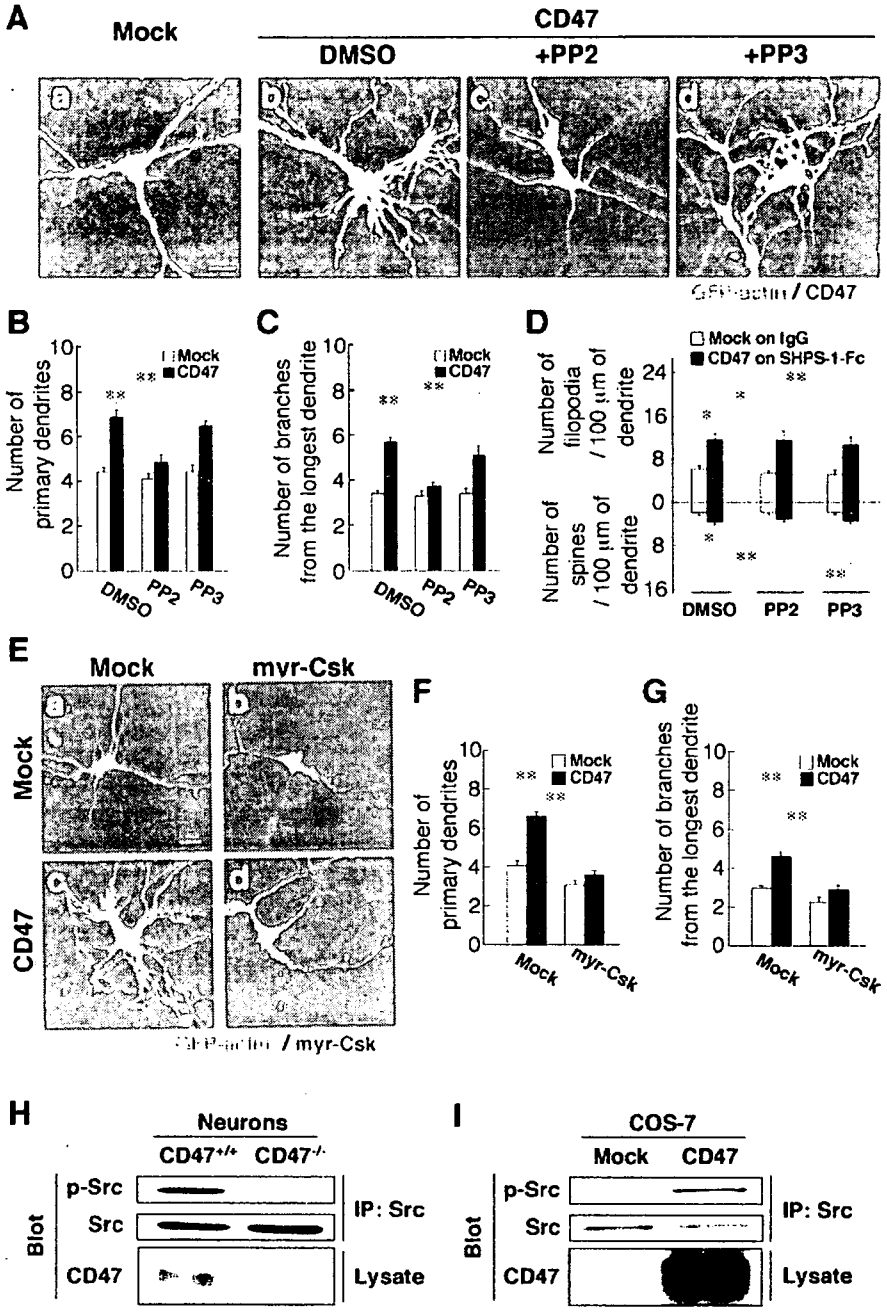

Figure 6. Participation of an Src family kinase in the promotion of dendritic development by CD47. ***A***, Hippocampal neurons from WT mice were transfected at 4 DIV with an expression vector for GFP–actin and either a vector for CD47 (***b–d***) or the corresponding empty vector (***a***). They were then cultured in the presence of 20 μM PP2 (***c***), 20 μM PP3 (***d***), or dimethylsulfoxide (DMSO) vehicle (***a***, ***b***). At 7 DIV, neurons were fixed and stained with an mAb to CD47 (red), and GFP–actin fluorescence was monitored (green). Scale bar, 20 μm. ***B–D***, The number of primary dendrites per neuron (***B***), that of branches from the longest primary dendrite of each neuron (***C***), and the density of dendritic filopodia or spines (***D***) were determined for neurons transfected and treated with PP2 or PP3 as in ***A***. In ***D***, neurons transfected with the CD47 vector were plated on SHPS-1–Fc, and those transfected with the corresponding empty vector were plated on human IgG. Data are means ± SE of values obtained from a total of 33–36 neurons (***B***, ***C***) or 28–32 neurons (***D***) in three independent experiments. $*p < 0.05$, $**p < 0.01$ (Student's *t* test). ***E***, Hippocampal neurons from WT mice were transfected at 4 DIV with an expression vector for GFP–actin, with either a vector for myr–Csk (***b***, ***d***) or the corresponding empty vector (***a***, ***c***), and with either a vector for CD47 (***c***, ***d***) or the corresponding empty vector (***a***, ***b***). At 7 DIV, neurons were fixed and stained with pAbs to Csk (red), and GFP–actin fluorescence was monitored (green). Neurons were also stained with an mAb to CD47 to confirm its expression (data not shown). Scale bar, 20 μm. ***F***, ***G***, The number of primary dendrites per neuron (***F***) and that of branches from the longest primary dendrite of each neuron (***G***) were determined for neurons treated as in ***E***. Data are means ± SE of values obtained from a total of 30 neurons in three independent experiments. $**p < 0.01$ (Student's *t* test). ***H***, Cultured hippocampal neurons from *CD47*$^{+/+}$ or *CD47*$^{-/-}$ mice were lysed at 7 DIV and subjected to immunoprecipitation (IP) with an mAb to c-Src. The resulting precipitates were subjected to immunoblot analysis both with pAbs to the Tyr^{416}-phosphorylated form of c-Src (p-Src) and with the mAb to c-Src. Cell lysates were also directly subjected to immunoblot analysis with pAbs to CD47. Data are representative of three independent experiments. ***I***, COS-7 cells were transfected with a vector for CD47 or the corresponding empty vector. Twenty-four hours after transfection, the cells were lysed and subjected to immunoprecipitation with an mAb to c-Src. The resulting precipitates as well as the original cell lysates were then subjected to immunoblot analysis as in ***H***. Data are representative of three independent experiments.

Role of an Src family kinase in dendritic development promoted by CD47

We next continued our attempt to identify downstream signaling molecules responsible for the promotion of dendritic development in hippocampal neurons by CD47. Treatment of neurons with PP2, an inhibitor of Src family kinases (Hanke et al., 1996), prevented the increases in the number of primary dendrites per neuron and branches from the longest primary dendrite induced by forced expression of CD47 in hippocampal neurons from WT mice; it did not affect these parameters in neurons not overexpressing CD47 (Fig. 6*Aa–Ac*, *B*, *C*). In addition, PP3, an inactive analog of PP2, did not inhibit these effects of CD47 (Fig. 6*Ad*, *B*, *C*). In contrast, PP2 and PP3 each failed to inhibit the formation of dendritic filopodia and spines induced by overexpression of CD47 and exposure to SHPS-1–Fc (Fig. 6*D*).

Csk inhibits the activity of Src family kinases by phosphorylating their COOH-terminal tyrosine residue (Honda et al., 1997). In addition, a membrane-targeted form of Csk (myr–Csk), which contains a myristylation signal at its NH_2 terminus, has been shown to inhibit the activity of Src family kinases more effectively than does wild-type Csk (Honda et al., 1997). Forced expression of myr–Csk prevented the increases in the number of primary dendrites per neuron and in the number of branches from the longest primary dendrite induced by forced expression of CD47, whereas it also reduced these parameters in neurons not overexpressing CD47 (Fig. 6*E–G*).

We then examined the effect of CD47 on the tyrosine phosphorylation state and activation of Src in hippocampal neurons. Activation of c-Src results in autophosphorylation of the enzyme on tyrosine-416 (Brown and Cooper, 1996). Immunoprecipitates prepared from lysates of WT or *CD47*$^{-/-}$ hippocampal neurons with an mAb to c-Src were subjected to immunoblot analysis with pAbs to the Tyr^{416}-phosphorylated form of c-Src. The phosphorylation of c-Src on Tyr^{416} was markedly reduced in *CD47*$^{-/-}$ neurons compared with that in WT neurons (Fig. 6*H*). Furthermore, forced expression of CD47 in COS-7 cells resulted in an in-

crease in the phosphorylation of c-Src on Tyr^{416} (Fig. 6*I*). Together, these data suggested that an Src family kinase mediates, at least in part, the promotion of dendritic development in hippocampal neurons by CD47.

Role of Vav2 and FRG in the promotion of dendritic development by CD47

Vav2, a GEF for Rho family proteins, is activated by Src-mediated tyrosine phosphorylation (Marignani and Carpenter, 2001; Servitja et al., 2003). In addition, FRG, another GEF specific for Cdc42 and Rac, undergoes tyrosine phosphorylation by c-Src and is thereby activated (Miyamoto et al., 2003; Fukuhara et al., 2004). Immunoblot analysis has revealed that both Vav2 and FRG are expressed in cultured hippocampal neurons (Kubo et al., 2002) (data not shown). We thus next examined whether Vav2 or FRG participates in CD47-induced dendritic development.

We first investigated the effects of forced expression of a dominant-negative mutant of Vav2 (Vav2–DN), in which Leu^{212} is replaced by Gln (Kodama et al., 2000; Kawakatsu et al., 2005). Forced expression of Vav2–DN, but not that of Vav2–WT, prevented the increases in both the number of primary dendrites per neuron and the number of branches from the longest primary dendrite induced by forced expression of CD47; it had no effect on these parameters in neurons not overexpressing CD47 (Fig. 7*A–C*). In contrast, forced expression of neither Vav2–DN nor Vav2–WT inhibited the increase in the density of dendritic filopodia and spines induced by CD47 overexpression and exposure to SHPS-1–Fc (Fig. 7*D*).

We next examined the effects of forced expression of a dominant-negative mutant of FRG (FRG-ΔDHPH), which lacks both the DH and PH domains of the intact protein (Miyamoto et al., 2003; Fukuhara et al., 2004). Expression of FRG–ΔDHPH prevented the increases in both the number of primary dendrites per neuron and the number of branches from the longest primary dendrite induced by forced expression of CD47; it had no effect on these parameters in neurons not overexpressing CD47 (supplemental Fig. 5*Ab,Ae,B,C*, available at www.jneurosci.org as supplemental material). However, forced expression of FRG–WT also prevented these effects of CD47 (supplemental Fig. 5*Af,B,C*). Forced expression of FRG–WT was shown previously to prevent neurite extension by cortical neurons (Kubo et al., 2002). We therefore examined the effect of depletion of endogenous FRG by RNA interference (RNAi) on the promotion of dendritic development by CD47. Transfection with an expression vector, siRNAfrg–GFP#2, for an siRNA specific for mouse FRG mRNA (nucleotides 2000–2018) resulted in a marked decrease in the amount of exogenously expressed mouse FRG in transfected HEK293 cells (Fig. 8*A*). Transfection of hippocampal neurons with the siRNAfrg–GFP#2 vector prevented the increases in both the number of primary dendrites per neuron and the number of branches from the longest primary dendrite induced by forced expression of CD47, without affecting these parameters in neurons not overexpressing CD47 (Fig. 8*B–D*). In contrast, transfection with siRNAfrg–GFP#2 failed to prevent the formation of dendritic filopodia and spines induced by overexpression of CD47 and exposure to SHPS-1–Fc (Fig. 8*E*). We also designed another expression vector, siRNAfrg–GFP#1, for an siRNA that targets a different region of mouse FRG mRNA (nucleotides 1138–1156). Transfection with siRNAfrg–GFP#1 reduced the amount of exogenous mouse FRG in transfected HEK293 cells and prevented the CD47-induced increases in both the number of primary dendrites per neuron and the number of branches from the longest primary dendrite in hippocampal neurons (data not shown).

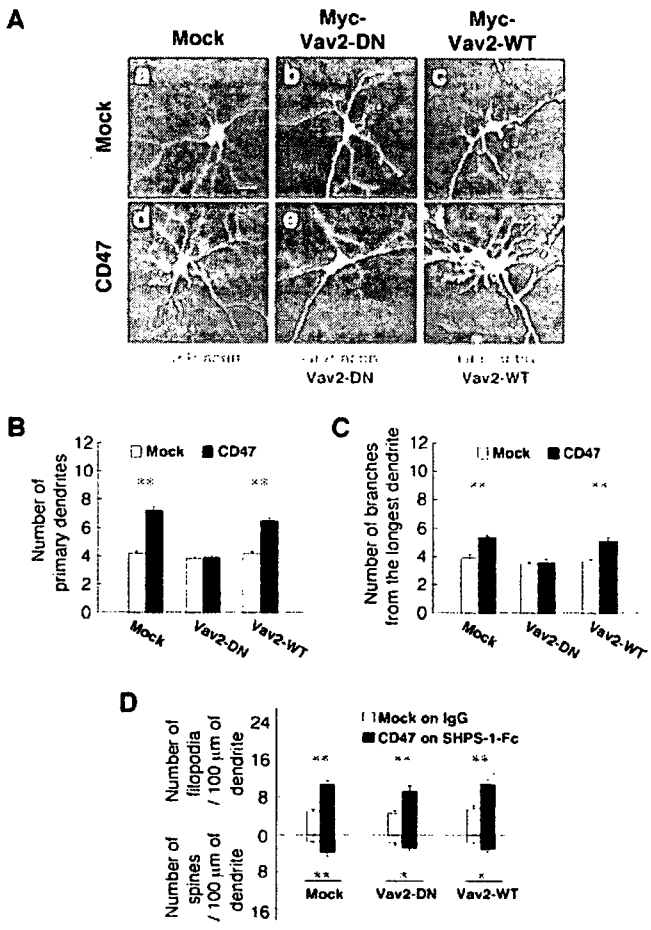

Figure 7. Participation of Vav2 in the promotion of dendritic development by CD47. ***A***, Hippocampal neurons from WT mice were transfected at 4 DIV with a vector for GFP–actin, a vector for CD47 (***d–f***) or the corresponding empty vector (***a–c***), and a vector for Myc epitope-tagged Vav2–DN (***b***, ***e***), a vector for Myc–Vav2–WT (***c***, ***f***), or the corresponding empty vector (***a***, ***d***). At 7 DIV, neurons were fixed and stained with an mAb to Myc (red), and GFP–actin fluorescence was monitored (green). Neurons were also stained with an mAb to CD47 to confirm its expression (data not shown). Scale bar, 20 μm. ***B***, ***C***, The number of primary dendrites per neuron (***B***) and that of branches from the longest primary dendrite of each neuron (***C***) were determined for neurons treated as in ***A***. Data are means ± SE of values obtained from a total of 30 neurons in three independent experiments. $^{**}p < 0.01$ (Student's *t* test). ***D***, Neurons transfected as in ***A*** were cultured on dishes coated with either SHPS-1–Fc (for those transfected with the CD47 vector) or control human IgG (for those transfected with the corresponding empty vector). At 7 DIV, they were fixed and stained with an mAb to Myc, and the densities of dendritic filopodia and spines were determined. Data are means ± SE of values obtained from a total of 18 neurons in three independent experiments. $^{*}p < 0.05$, $^{**}p < 0.01$ (Student's *t* test).

Discussion

We have shown that CD47 promotes dendritic and axonal development in hippocampal neurons. Loss of CD47 impaired the formation of dendrites and their branching, whereas forced expression of this protein restored and further promoted dendritic development in cultured $CD47^{-/-}$ neurons. In addition, deficiency of CD47 impaired the elongation of axons and their branching as well as the formation of growth cones. The impairment in dendritic development of $CD47^{-/-}$ hippocampal neurons was evident at an early stage of culture (3–7 DIV) but not at later stages (14–21 DIV). Forced expression of CD47 also increased the number and branching of dendrites in WT neurons at

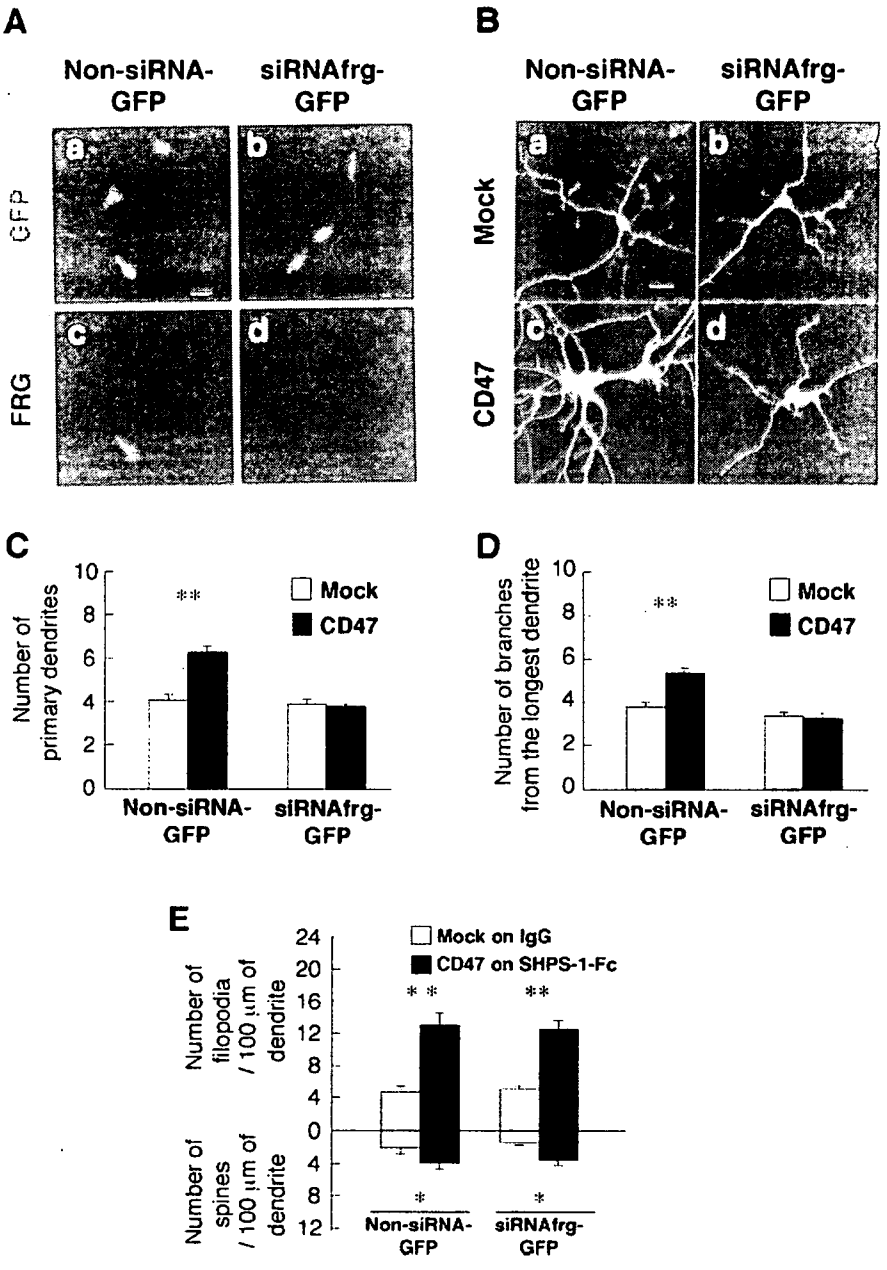

Figure 8. Effects of RNAi-mediated depletion of FRG on CD47-induced dendritic development. ***A***, HEK293 cells were transfected with an expression vector for mouse FRG and either siRNAfrg–GFP#2 (***b***, ***d***) or the corresponding GFP vector (Non-siRNA-GFP; ***a***, ***c***). Forty-eight hours after transfection, the cells were fixed and stained with pAbs to FRG (***c***, ***d***) and monitored for GFP fluorescence (***a***, ***b***). Scale bar, 20 μm. ***B***, Hippocampal neurons from WT mice were transfected at 4 DIV with siRNAfrg–GFP#2 (***b***, ***d***) or the corresponding GFP vector (***a***, c), as well as with a vector for CD47 (***c***, ***d***) or the corresponding empty vector (***a***, ***b***). Neurons were fixed, and the expression of GFP was monitored at 7 DIV. Neurons were also stained with an mAb to CD47 (data not shown). Scale bar, 20 μm. ***C***, ***D***, The number of primary dendrites per neuron (***C***) and that of branches from the longest primary dendrite of each neuron (***D***) were determined for neurons treated as in ***B***. Data are means ± SE of values from a total of 20–30 neurons in three independent experiments. $^{**}p < 0.01$ (Student's *t* test). ***E***, Hippocampal neurons from WT mice were transfected as in ***B*** and cultured on dishes coated with either SHPS-1–Fc (for those transfected with the CD47 vector) or control human IgG (for those transfected with the corresponding empty vector). At 7 DIV, neurons were fixed and stained with an mAb to CD47, and the densities of dendritic filopodia and spines were determined. Data are means ± SE of values obtained from a total of 18 neurons in three independent experiments. $^{*}p < 0.05$, $^{**}p < 0.01$ (Student's *t* test).

3–7 DIV but not at 14–21 DIV. These results suggest that CD47 efficiently promotes dendritic and axonal development, in particular, at the early stage of formation of neuronal networks.

We also found that SHPS-1–Fc markedly promoted the formation of dendritic filopodia and spines in CD47-overexpressing hippocampal neurons at 7 DIV but not at 14 or 21 DIV. Given that formation of dendritic filopodia precedes that of dendritic spines (Ziv and Smith, 1996), these results further suggest that CD47, through its interaction with SHPS-1, promotes filopodium formation, resulting in efficient formation of spines and subsequent formation of synapses. We have shown previously that CD47 is localized predominantly to the surface of dendrites in hippocampal neurons, whereas SHPS-1 was detected at the surface of both axons and dendrites (Ohnishi et al., 2005). On the basis of our present results, we suggest that CD47 promotes the formation of filopodia on dendrites through its interaction with SHPS-1 expressed on neighboring axons, thereby contributing to subsequent formation of mature dendritic spines particularly at the early stage of development of neuronal networks. In contrast, because the effect of SHPS-1–Fc on filopodium or spine formation was not apparent at the later stage of culture (14 or 21 DIV), the functional role of engagement of SHPS-1 with CD47 after formation and maturation of neuronal networks remains unknown. However, synaptic connections between neurons are thought to be actively disrupted and reconnected even in mature CNS (De Paola et al., 2006; Stettler et al., 2006). Therefore, it is feasible that engagement of SHPS-1 with CD47 participates in the dendrite plasticity of neurons through regulation of formation of filopodia or spines. SHPS-1–Fc failed to increase the number of primary dendrites or that of branches from the longest primary dendrite in either mock-transfected or CD47-expressing neurons at 7 DIV (supplemental Fig. 3, available at www.jneurosci.org as supplemental material). These data indicate that engagement by CD47 of SHPS-1 is unlikely to promote dendrite formation and branching.

CD47$^{-/-}$ mice exhibit impaired memory retention and defective long-term potentiation (Chang et al., 1999). Such phenotypes might be attributable to impairment of dendritic and axonal development resulting from the loss of CD47. In contrast to our observations with cultured hippocampal neurons, we did not find marked impairment of dendritic or axonal development in *CD47*$^{-/-}$ hippocampus *in vivo*, whereas the branching of dendrites of hippocampal neurons at mutant mice at P0–P1 was slightly impaired *in vivo* by staining of fixed hippocampal sections with 1,1′-dioctadecyl-3,3,3′,3′-tetramethylindocarboyanine perchlorate (data not shown).

We also shown that inhibition of Rac or Cdc42 prevented the effects of forced expression of CD47 on the formation of dendrites and their branching in cultured hippocampal neurons.

Moreover, we showed that either Rac or Cdc42 in hippocampal neurons are indeed activated by forced expression of CD47 by the use of FRET imaging. We showed previously that forced expression of CD47 also induced a marked increase of the activity of Rac or Cdc42 in COS-7 cells by the use of pull-down assay (Miyashita et al., 2004). Together, our results suggest that Rac as well as Cdc42 participate in the signaling downstream of CD47 in hippocampal neurons. The formation of dendritic filopodia and spines induced by SHPS-1–Fc in CD47-overexpressing neurons was also prevented by inhibition of Cdc42. These data are also consistent with our previous observations in the neuroblastoma cell line N1E-115 (Miyashita et al., 2004). Rac and Cdc42 are thought to regulate axonal or dendritic development in neurons through their effects on the arrangement of the actin cytoskeleton (Luo et al., 1997; Takai et al., 2001; Govek et al., 2005). However, it has remained unclear which cell surface proteins participate in coupling of extracellular stimuli to activation of these small GTP-binding proteins in such regulation. Our data now suggest that CD47 is such a protein in hippocampal neurons.

Our data have also provided insight into the signaling pathway that links CD47 to Rac or Cdc42 in hippocampal neurons. Inhibition by PP2 or Csk of an Src family kinase prevented the promotion of dendritic development by CD47. In addition, loss of CD47 markedly reduced the activation of c-Src in hippocampal neurons, whereas forced expression of CD47 induced activation of this kinase. These results suggest that c-Src or another Src family kinase participates in CD47-induced dendritic development. The mechanism by which CD47 promotes activation of an Src family kinase is unknown. CD47 interacts with integrins through its extracellular region and participates in integrin-mediated biological responses in non-neural cells (Brown and Frazier, 2001). Various integrin subunits, including αv, $\alpha 2$, $\alpha 5$, $\beta 1$, and $\beta 3$, are expressed in the hippocampus (Bi et al., 2001; Chan et al., 2003). In addition, integrin engagement induces recruitment and subsequent activation of c-Src, which in turn phosphorylates downstream signaling molecules (Brunton et al., 2004). CD47 may thus induce activation of c-Src through its interaction with integrins in hippocampal neurons. Unexpectedly, however, inhibition of integrin signaling by echistatin or mAbs to integrin $\beta 1$ or $\beta 3$ subunits failed to prevent the stimulatory effect of CD47 on dendritic development in hippocampal neurons (data not shown). It is thus possible that CD47 induces activation of c-Src in an integrin-independent manner in hippocampal neurons. Indeed, CD47 was shown previously to promote T-cell activation in a manner independent of integrins (Reinhold et al., 1997).

Inhibition of either Vav2 or FRG prevented the promotion of dendritic development by CD47. Vav2 activates Rac and Cdc42 (Abe et al., 2000; Marignani and Carpenter, 2001), as does FRG (Kubo et al., 2002; Miyamoto et al., 2003; Fukuhara et al., 2004). Our results thus suggest that Vav2 and FRG participate in the stimulatory effect of CD47 on dendritic development in hippocampal neurons. Given that both of these GEFs are activated as a result of tyrosine phosphorylation by c-Src (Marignani and Carpenter, 2001; Miyamoto et al., 2003; Servitja et al., 2003), it is most likely that the activation of c-Src by CD47 results in the tyrosine phosphorylation and activation of Vav2 and FRG in hippocampal neurons. In contrast, it is also possible that Src, Vav2, and FRG may act in parallel. The promotion of filopodium and spine formation by CD47 and SHPS-1–Fc was not prevented by inhibition of Src, Vav2, or FRG, however, suggesting that another as yet unidentified GEF for Cdc42 participates in this effect of CD47 and SHPS-1–Fc. We also tested the effects of a dominant-negative mutant of Tiam1 (T-cell lymphoma invasion and metastasis 1), another GEF for Rac (Michiels et al., 1997). However, expression of this mutant failed to prevent the CD47-induced increases in the number of primary dendrites per neuron and branches from the longest primary dendrite (data not shown). It also failed to prevent the formation of dendritic filopodia and spines induced by CD47 and SHPS-1–Fc (data not shown).

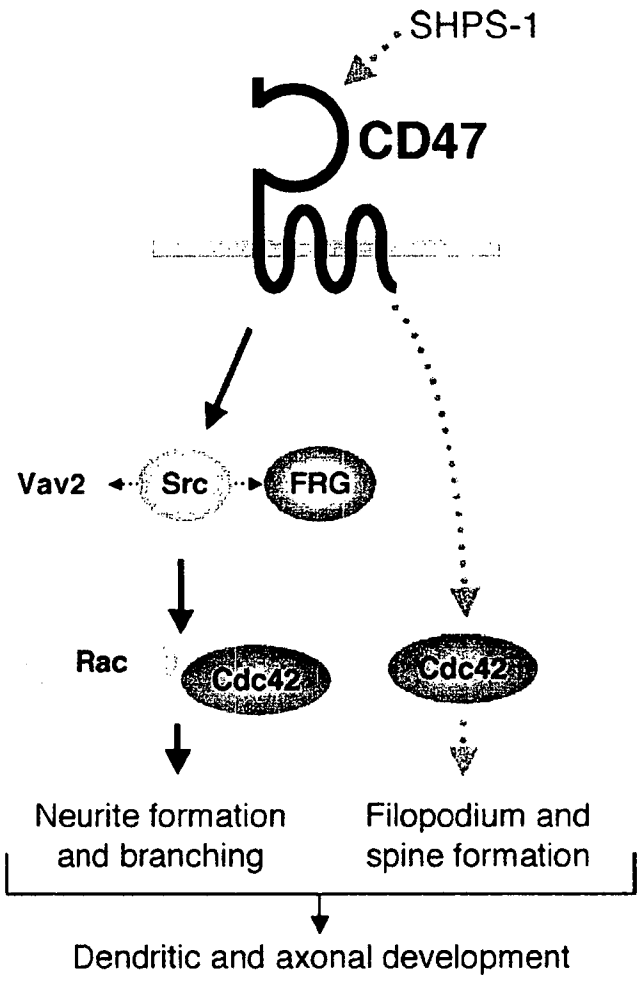

Figure 9. Model for the promotion of neuronal development by CD47. The activation by CD47 of an Src family kinase may result in the tyrosine phosphorylation of Vav2 and FRG, the consequent activation of Rac and Cdc42, and the promotion of neurite formation and branching. Src, Vav2, and FRG may also act in parallel at the signaling downstream of CD47. Interaction of SHPS-1 with CD47 promotes the formation of dendritic filopodia and spines possibly through a different signaling pathway involving Cdc42 (dotted green lines), although the mechanism of such an effect is unknown.

In summary, we propose the following model for the mode of CD47 action in the promotion of dendritic and axonal development in hippocampal neurons (Fig. 9). CD47 activates an Src family kinase, such as c-Src, directly or indirectly, which likely results in the tyrosine phosphorylation of Vav2 and FRG and the consequent activation of Rac and Cdc42. Alternatively, Src, Vav2, and FRG may also act in parallel at the signaling downstream of CD47. Interaction of SHPS-1 with CD47 promotes the formation of dendritic filopodia and spines potentially through activation of Cdc42, although the mechanism for such activation is unknown.

References

Abe K, Rossman KL, Liu B, Ritola KD, Chiang D, Campbell SL, Burridge K, Der CJ (2000) Vav2 is an activator of Cdc42, Rac1, and RhoA. J Biol Chem 275:10141–10149.

Bi X, Lynch G, Zhou J, Gall CM (2001) Polarized distribution of alpha5 integrin in dendrites of hippocampal and cortical neurons. J Comp Neurol 435:184–193.

Brown EJ, Frazier WA (2001) Integrin-associated protein (CD47) and its ligands. Trends Cell Biol 11:130–135.

Brown MT, Cooper JA (1996) Regulation, substrates and functions of src. Biochim Biophys Acta 1287:121–149.

Brummelkamp TR, Bernards R, Agami R (2002) A system for stable expression of short interfering RNAs in mammalian cells. Science 296:550–553.

Brunton VG, MacPherson IR, Frame MC (2004) Cell adhesion receptors, tyrosine kinases and actin modulators: a complex three-way circuitry. Biochim Biophys Acta 1692:121–144.

Chan CS, Weeber EJ, Kurup S, Sweatt JD, Davis RL (2003) Integrin requirement for hippocampal synaptic plasticity and spatial memory. J Neurosci 23:7107–7116.

Chang HP, Lindberg FP, Wang HL, Huang AM, Lee EH (1999) Impaired memory retention and decreased long-term potentiation in integrin-associated protein-deficient mice. Learn Mem 6:448–457.

De Paola V, Holtmaat A, Knott G, Song S, Wilbrecht L, Caroni P, Svoboda K (2006) Cell type-specific structural plasticity of axonal branches and boutons in the adult neocortex. Neuron 49:861–875.

Dickson BJ (2002) Molecular mechanisms of axon guidance. Science 298:1959–1964.

Fujioka Y, Matozaki T, Noguchi T, Iwamatsu A, Yamao T, Takahashi N, Tsuda M, Takada T, Kasuga M (1996) A novel membrane glycoprotein, SHPS-1, that binds the SH2-domain-containing protein tyrosine phosphatase SHP-2 in response to mitogens and cell adhesion. Mol Cell Biol 16:6887–6899.

Fukuhara T, Shimizu K, Kawakatsu T, Fukuyama T, Minami Y, Honda T, Hoshino T, Yamada T, Ogita H, Okada M, Takai Y (2004) Activation of Cdc42 by trans interactions of the cell adhesion molecules nectins through c-Src and Cdc42-GEF FRG. J Cell Biol 166:393–405.

Govek EE, Newey SE, Van Aelst L (2005) The role of the Rho GTPases in neuronal development. Genes Dev 19:1–49.

Hanke JH, Gardner JP, Dow RL, Changelian PS, Brissette WH, Weringer EJ, Pollok BA, Connelly PA (1996) Discovery of a novel, potent, and Src family-selective tyrosine kinase inhibitor. Study of Lck- and FynT-dependent T cell activation. J Biol Chem 271:695–701.

Honda Z, Suzuki T, Hirose N, Aihara M, Shimizu T, Nada S, Okada M, Ra C, Morita Y, Ito K (1997) Roles of C-terminal Src kinase in the initiation and the termination of the high affinity IgE receptor-mediated signaling. J Biol Chem 272:25753–25760.

Huang AM, Wang HL, Tang YP, Lee EH (1998) Expression of integrin-associated protein gene associated with memory formation in rats. J Neurosci 18:4305–4313.

Itoh RE, Kurokawa K, Ohba Y, Yoshizaki H, Mochizuki N, Matsuda M (2002) Activation of Rac and Cdc42 video imaged by fluorescent resonance energy transfer-based single-molecule probes in the membrane of living cells. Mol Cell Biol 22:6582–6591.

Jan YN, Jan LY (2003) The control of dendrite development. Neuron 40:229–242.

Jiang P, Lagenaur CF, Narayanan V (1999) Integrin-associated protein is a ligand for the P84 neural adhesion molecule. J Biol Chem 274:559–562.

Kawakatsu T, Ogita H, Fukuhara T, Fukuyama T, Minami Y, Shimizu K, Takai Y (2005) Vav2 as a Rac-GDP/GTP exchange factor responsible for the nectin-induced, c-Src- and Cdc42-mediated activation of Rac. J Biol Chem 280:4940–4947.

Kodama A, Matozaki T, Fukuhara A, Kikyo M, Ichihashi M, Takai Y (2000) Involvement of an SHP-2-Rho small G protein pathway in hepatocyte growth factor/scatter factor-induced cell scattering. Mol Biol Cell 11:2565–2575.

Kubo T, Yamashita T, Yamaguchi A, Sumimoto H, Hosokawa K, Tohyama M (2002) A novel FERM domain including guanine nucleotide exchange factor is involved in Rac signaling and regulates neurite remodeling. J Neurosci 22:8504–8513.

Lindberg FP, Bullard DC, Caver TE, Gresham HD, Beaudet AL, Brown EJ (1996) Decreased resistance to bacterial infection and granulocyte defects in IAP-deficient mice. Science 274:795–798.

Luo L, Jan LY, Jan YN (1997) Rho family GTP-binding proteins in growth cone signalling. Curr Opin Neurobiol 7:81–86.

Marignani PA, Carpenter CL (2001) Vav2 is required for cell spreading. J Cell Biol 154:177–186.

Mi ZP, Jiang P, Weng WL, Lindberg FP, Narayanan V, Lagenaur CF (2000) Expression of a synapse-associated membrane protein, P84/SHPS-1, and its ligand, IAP/CD47, in mouse retina. J Comp Neurol 416:335–344.

Michiels F, Stam JC, Hordijk PL, van der Kammen RA, Ruuls-Van Stalle L, Feltkamp CA, Collard JG (1997) Regulated membrane localization of Tiam1, mediated by the NH2-terminal pleckstrin homology domain, is required for Rac-dependent membrane ruffling and C-Jun NH2-terminal kinase activation. J Cell Biol 137:387–398.

Miyamoto Y, Yamauchi J, Itoh H (2003) Src kinase regulates the activation of a novel FGD-1-related Cdc42 guanine nucleotide exchange factor in the signaling pathway from the endothelin A receptor to JNK. J Biol Chem 278:29890–29900.

Miyashita M, Ohnishi H, Okazawa H, Tomonaga H, Hayashi A, Fujimoto TT, Furuya N, Matozaki T (2004) Promotion of neurite and filopodium formation by CD47: roles of integrins, Rac, and Cdc42. Mol Biol Cell 15:3950–3963.

Ohnishi H, Kubota M, Ohtake A, Sato K, Sano S (1996) Activation of protein-tyrosine phosphatase SH-PTP2 by a tyrosine-based activation motif of a novel brain molecule. J Biol Chem 271:25569–25574.

Ohnishi H, Kaneko Y, Okazawa H, Miyashita M, Sato R, Hayashi A, Tada K, Nagata S, Takahashi M, Matozaki T (2005) Differential localization of Src homology 2 domain-containing protein tyrosine phosphatase substrate-1 and CD47 and its molecular mechanisms in cultured hippocampal neurons. J Neurosci 25:2702–2711.

Polleux F, Morrow T, Ghosh A (2000) Semaphorin 3A is a chemoattractant for cortical apical dendrites. Nature 404:567–573.

Reinhold MI, Lindberg FP, Plas D, Reynolds S, Peters MG, Brown EJ (1995) In vivo expression of alternatively spliced forms of integrin-associated protein (CD47). J Cell Sci 108:3419–3425.

Reinhold MI, Lindberg FP, Kersh GJ, Allen PM, Brown EJ (1997) Costimulation of T cell activation by integrin-associated protein (CD47) is an adhesion-dependent, CD28-independent signaling pathway. J Exp Med 185:1–11.

Servitja JM, Marinissen MJ, Sodhi A, Bustelo XR, Gutkind JS (2003) Rac1 function is required for Src-induced transformation. Evidence of a role for Tiam1 and Vav2 in Rac activation by Src. J Biol Chem 278:34339–34346.

Shamah SM, Lin MZ, Goldberg JL, Estrach S, Sahin M, Hu L, Bazalakova M, Neve RL, Corfas G, Debant A, Greenberg ME (2001) EphA receptors regulate growth cone dynamics through the novel guanine nucleotide exchange factor ephexin. Cell 105:233–244.

Stettler DD, Yamahachi H, Li W, Denk W, Gilbert CD (2006) Axons and synaptic boutons are highly dynamic in adult visual cortex. Neuron 49:877–887.

Takahashi H, Sekino Y, Tanaka S, Mizui T, Kishi S, Shirao T (2003) Drebrin-dependent actin clustering in dendritic filopodia governs synaptic targeting of postsynaptic density-95 and dendritic spine morphogenesis. J Neurosci 23:6586–6595.

Takai Y, Sasaki T, Matozaki T (2001) Small GTP-binding proteins. Physiol Rev 81:153–208.

Tessier-Lavigne M, Goodman CS (1996) The molecular biology of axon guidance. Science 274:1123–1133.

Wahl S, Barth H, Ciossek T, Aktories K, Mueller BK (2000) Ephrin-A5 induces collapse of growth cones by activating Rho and Rho kinase. J Cell Biol 149:263–270.

Whitford KL, Marillat V, Stein E, Goodman CS, Tessier-Lavigne M, Chedotal A, Ghosh A (2002) Regulation of cortical dendrite development by Slit-Robo interactions. Neuron 33:47–61.

Ziv NE, Smith SJ (1996) Evidence for a role of dendritic filopodia in synaptogenesis and spine formation. Neuron 17:91–102.

ELSEVIER

Auris Nasus Larynx 32 (2005) 33–37

AURIS NASUS LARYNX
INTERNATIONAL JOURNAL OF ORL & HNS

www.elsevier.com/locate/anl

Inhibition of caspases alleviates gentamicin-induced cochlear damage in guinea pigs

Takeshi Okuda, Kazuma Sugahara, Tsuyoshi Takemoto, Hiroaki Shimogori, Hiroshi Yamashita*

Department of Otolaryngology, Yamaguchi University School of Medicine, Minamikogushi 1-1-1, Ube, Yamaguchi, Japan

Received 22 June 2004; received in revised form 12 October 2004; accepted 26 November 2004
Available online 26 January 2005

Abstract

The efficacy of caspase inhibitors for protecting the cochlea was evaluated in an in vivo study using guinea pigs, as the animal model system. Gentamicin (12 mg/ml) was delivered via an osmotic pump into the cochlear perilymphatic space of guinea pigs at 0.5 μl/h for 14 days. Additional animals were given either z-Val-Ala-Asp (Ome)-fluoromethyl ketone (z-VAD-FMK) or z-Leu-Glu-His-Asp-FMK (z-LEHD-FMK), a general caspase inhibitor and a caspase 9 inhibitor, respectively, in addition to gentamicin. The elevation in auditory brain stem response thresholds, at 4, 7, and 14 days following gentamicin administration, were decreased in animals that received both z-VAD-FMK and z-LEHD-FMK. Cochlear sensory hair cells survived in greater numbers in animals that received caspase inhibitors in addition to gentamicin, whereas sensory hair cells in animals that received gentamicin only were severely damaged. These results suggest that auditory cell death induced by gentamicin is closely related to the activation of caspases in vivo.

Keywords: Inner ear; Hair cell; Aminoglycoside; Caspase; Guinea pig

1. Introduction

The cochlea is unlikely, under normal circumstances, to be exposed to outside stresses, as the inner ear is enclosed by a bony wall and separated from blood by the blood–inner ear barrier. However, cochlear hair cells are quite easily damaged by specific chemical compounds [1,15], elevated noise levels [11,12,19] and ischemia [3]. There have been many cases of hearing loss as a result of these stresses. Aminoglycosides are a class of compounds that are well known as specific ototoxic agents [28,29], and recent research has suggested that hair cell death induced by these chemicals is closely related to apoptosis. In a 1985 study, Forge and co-workers [7,8] reported morphologic evidence of aminoglycoside-induced sensory hair cell apoptosis. In addition, the organ culture studies have provided evidence of an apoptotic cell death pathway in the inner ear. Matsui et al. [16] reported that caspase inhibitors suppressed apoptosis induced by aminoglycosides, and Cunningham et al. [6] reported that caspase 9 was more effective than caspase 8 at promoting apoptosis of hair cells. Recently, Matsui et al. [17] showed that either systemic or local application of general caspase inhibitor could protect chick vestibular sensory cells against the aminoglycoside-induced cell death in vivo. These evidences indicated that caspase signaling pathway has an important role in the aminoglycoside induced hair cell death, and that the inhibition of caspases may be one of the candidates for the treatment of inner ear diseases involving hair cell death. However, it has been unclear whether the effect of caspase inhibitor can protect hair cells of the mammals in vivo. Therefore, we planned to administrate the specific inhibitor of caspase 9 as well as the general caspase inhibitor into the cochlea of guinea pigs. The aim of this present study was to determine the effect of caspase inhibitors on cochlear hair cell death of mammals induced by aminoglycosides.

* Corresponding author. Tel.: +81 836 22 2281; fax: +81 836 22 2280.
E-mail address: hiro-shi@yamaguchi-u.ac.jp (H. Yamashita).

0385-8146/$ – see front matter
doi:10.1016/j.anl.2004.11.006

2. Materials and methods

2.1. Animal subjects and experimental design

The experimental animals incorporated into this study were 15 male Hartley guinea pigs (350–400 g) with Preyer's reflexes and normally appearing tympanic membranes. All experimental protocols were reviewed by the Committee for Ethics on Animal Experiments at the Yamaguchi University School of Medicine. Experiments were carried out in accordance with the University Guidelines, Japanese Federal Law (No. 105) and Notification No. 6 of the Japanese Government.

The study protocol is described schematically in Fig. 1. Osmotic pumps (Model 2002, Alza Co., Palo Alto, CA, USA) filled with sterile saline were implanted into each animal for the infusion of agents into the right cochlear perilymphatic space. The procedures for implantation of osmotic pumps were performed on the right ears, and the intact left ears were used for control. Seven days after pump implantation each osmotic pump was newly replaced with a pump containing the specific agent to be delivered in combination with gentamicin. The animals were then divided into three groups ($n = 5$ in each) according to the contents of the replacement pumps (agents were infused at a rate of 0.5 μl/h for 14 days in each case); GM only group received a 12 mg/ml gentamicin solution (Schering-Plough K.K., Kenilworth, NJ, USA) in 1% dimethyl sulfoxide (DMSO) (Sigma, St. Louis, MO, USA) with saline; GM + general caspase inhibitor group received a gentamicin solution (12 mg/ml) containing 250 μM of the general caspase inhibitor (z-Val-Ala-Asp (Ome)-fluoromethyl ketone (z-VAD-FMK) (Enzyme System Products, Livemore, CA, USA) also in 1% DMSO with saline; GM + caspase 9 inhibitor group received a gentamicin solution (12 mg/ml) containing 250 μM of the caspase 9 inhibitor (z-Leu-Glu-His-Asp-FMK (z-LEHD-FMK) (Kamiya Biomedical Company, Seattle, WA, USA) in 1% DMSO with saline. To evaluate cochlear function, auditory brain stem response (ABR) thresholds were assessed before and at 4-, 7- and 14-day time points following the exchange of osmotic pumps. Following the final ABR examination, each of the animals was sacrificed for histological examination.

2.2. Implantation and exchange of osmotic pumps

For the infusion of specific agents into the inner ears of the experimental animals, we used osmotic pumps connected to 10 cm polyethylene catheters (i.d. = 0.28 mm, o.d. = 0.61 mm) and a 1 mm Teflon catheter (i.d. = 0.18 mm, o.d. = 0.3 mm) with plastic glue. Both pumps and catheters were infused with sterile saline and were pretreated in saline until implantation. The surgical procedures for the pump implantations were performed under general anesthesia with ketamine (16 mg/kg, intraperitoneal injection (i.p.)) and xylazine (16 mg/kg, i.p.) and local anesthesia (1% lidocaine HCl, 1.5 ml). The mastoid bulla was exposed via postauricular incision at the right ear, and two incisions were then made into it with a small electric drill for both the procedure and subsequent observations. A tiny hole was then made on the cochlear bony wall at a distance of 1 mm from the round window with a fine needle. The hole was sized to fit the catheter. The tip of the catheter, which was connected to the osmotic pump, was inserted into the perilymphatic space of the cochlear basal turn via this tiny hole. We subsequently confirmed that the perilymph did not leak out. The catheter was fixed to the mastoid bulla with dental cement (GC Fuji1, GC Co., Tokyo, Japan). After the skin incision was closed, antibiotic ointment was applied. All animals received sterile saline at 0.5 μl/h via right cochlear perilymph after implantation of osmotic pumps.

Osmotic pumps were exchanged for new pumps containing specific experimental reagents 7 days after implantation. The procedures for the exchange of pumps were performed under the same anesthesia used for the initial pump implantation. A new incision was then made at the back of the animals, and the first osmotic pump and catheter were

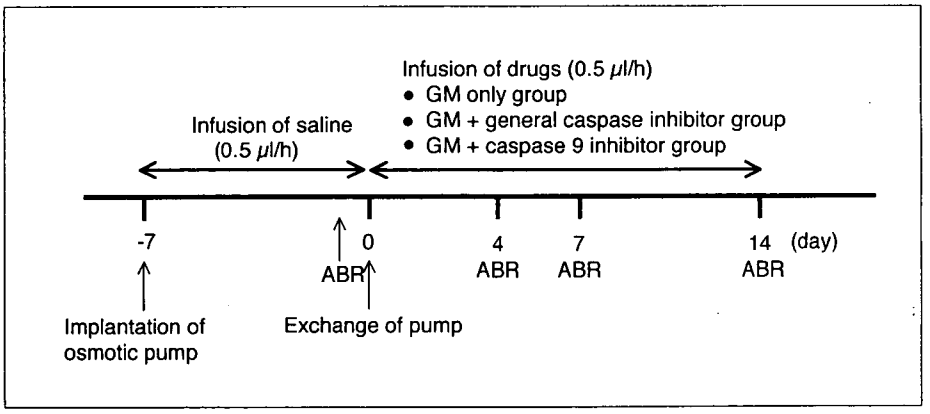

Fig. 1. Schematic depiction of the experimental protocol. Solutions containing gentamicin either alone or in combination with specific caspase inhibitors were administered for up to 14 days after the exchange of osmotic pumps. An ABR examination was performed prior to the exchange of the osmotic pump and at 4-, 7- and 14-day timepoints following the start of the infusion of agents.

exposed. The polyethylene catheter was then cut and connected to the new osmotic pump with plastic glue, and the incision was closed.

2.3. Assessment of auditory function

To evaluate auditory function, ABR thresholds were assessed under xylazine (16 mg/kg, i.p.) and ketamine (16 mg/kg, i.p.) anesthesia. Responses were recorded between subcutaneous stainless steel electrodes at the vertex (positive) and the antinion (negative), with the lower back of the animal serving as a ground. The sound stimuli consisted of 8 ms tone bursts with a rise-fall time of 2 ms at frequencies of 8 kHz and were presented via a 10 cm tube connecting an earphone to the external auditory canal. Responses to 500 stimuli were recorded by means of a signal processor (Synax 1100, NEC Co, Tokyo, Japan). The ABR threshold was defined as the lowest stimulus intensity that produced a reliable peak of III or V ABR waveforms. ABR threshold data from each animal were analyzed with Stat View version 4.5 J for the Macintosh (SAS Institute, Cary, NC, USA). The ABR threshold values in each group were compared using the Mann–Whitney's U-test, and a level of $P < 0.05$ was considered statistically significant.

2.4. Histological examination

On the last day of the protocol, the animals were sacrificed by pentobarbital overdose, and each of the cochleae were removed, gently perfused and incubated with fixative (4% paraformaldehyde in 0.01 M phosphate-buffered saline (PBS), pH 7.3) for 12 h and rinsed in PBS. The organs of Corti were then removed, permeabilized with 0.3% Triton X-100 for 10 min and incubated with fluorescein isothiocynate-conjugated phalloidin (1 μg/ml; Sigma, St. Louis, MO, USA) at room temperature for 1 h and rinsed in PBS. The surface structures was visualized by fluorescence microscopy (Nikon, Tokyo, Japan).

3. Results

Seven days after implantation of the osmotic pumps, the ABR thresholds of surgically treated ears were not found to be altered when compared with intact ears from each group (Fig. 2). Following the exchange of osmotic pumps, the ABR thresholds of GM only group and GM + general caspase inhibitor group gradually increased for 14 days. However, the rate of the increase in GM + general caspase inhibitor group was slower than that of GM only group and the ABR threshold values in GM + general caspase inhibitor group were also less than GM only group at each of the measured time points (4, 7 and 14 days) following the infusion of reagents. Similarly, the threshold shifts in GM + caspase 9 inhibitor group were also less than GM only group. These findings indicated that both the general caspase inhibitor and

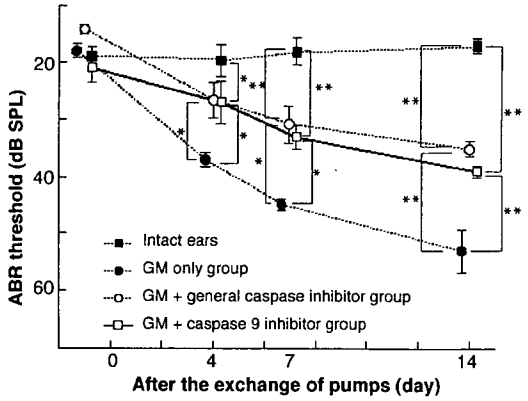

Fig. 2. Measurement of auditory brainstem response (ABR) thresholds in both control and treated ears. ABR thresholds increased gradually in each group during the infusion of gentamicin solutions. The thresholds in GM + general caspase inhibitor group and GM + caspase 9 inhibitor group increased at a slower rate than in GM only group and threshold shifts of greater than 20 dB were prevented in each of the experiments. Intact ears mean left ears that did not receive osmotic pump implantation; error bar, ±1S.E.; $*P < 0.05$; $**P < 0.01$.

caspase 9-specific inhibitor protected auditory functions against gentamicin ototoxicity.

The surface structures of the organ of Corti were examined at the end of the experimental protocol (Fig. 3). The certain part of third turn in each cochlea was used for the histological examination, because the procedure for the osmotic pump implantation might affect the surface structures near the basal turn. Though the outer hair cells had almost disappeared in the third turns in GM only group animals, a portion of these cells were still evident in GM + general caspase inhibitor group. In addition, many residual outer hair cells were present in GM + caspase 9 inhibitor group subjects. Inner hair cells were not affected in the cochlear third turn in any of the groups. These findings indicate that caspase inhibitors prevent outer hair cell death following exposure to gentamicin.

4. Discussion

In vitro experiments with inner ear tissue had previously suggested that sensory hair cells are protected by caspase inhibitors. In addition, the protective effects of caspase inhibitors were recently reported using the chick vestibular tissues in vivo [17]. However, the effects of the caspase inhibitors on the auditory hair cells of mammals in vivo have not been reported. In this study, we showed that caspase inhibitors prevented the hair cell death induced by gentamicin and protected the auditory functions of the subject animals using the mammal's cochlea. These findings indicate therefore that the activation of caspases plays an important role in pathways leading to cochlear hair cell death in mammals.

There are at least two major pathways through which apoptosis is induced: one involves death receptors and is

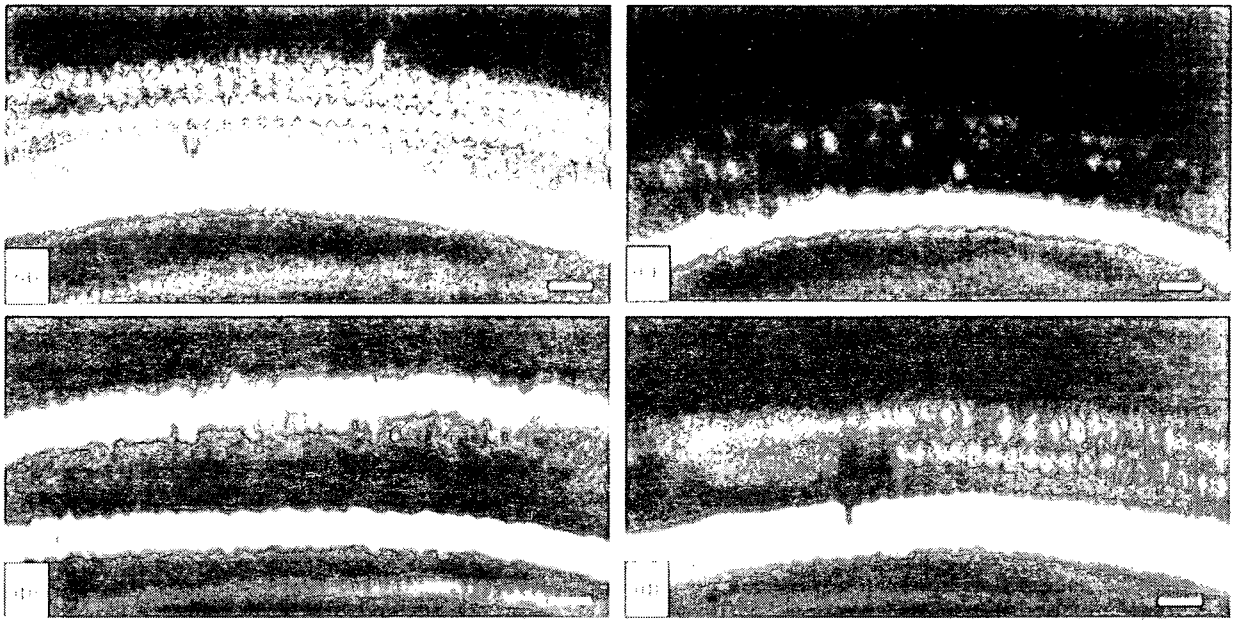

Fig. 3. Images of surface structures of the organ of Corti in the cochlear third turn 14 days after the administration of drugs. Actin filaments were stained with FITC-conjugated phalloidin to visualize sensory hair cells. In intact ear controls, a row of inner hair cells and three rows of outer hair cells were evident (a). Fluorescence microscopy revealed a severe reduction in outer hair cells in GM only group (b); although residual outer hair cells were observed in GM + general caspase inhibitor group (c) and GM + caspase 9 inhibitor group (d); bar = 20 μm.

exemplified by Fas-mediated caspase 8 activation, and another is the stress- or mitochondria-mediated caspase 9 activation pathway [2,22,27,30]. These caspases activate downstream caspases, such as caspase 3 and results in nuclear degradation and cellular morphological change. The recent in vitro study indicated that the caspase 9 activation pathway have more important role in the hair cell death induced by aminoglycosides than caspase 8 activation pathway [6]. Therefore, we used the specific inhibitor of caspase 9 as well as the general caspase inhibitor. In the study, z-VAD-FMK was used as the general caspase inhibitor. The reagent has the inhibition activities against at least caspase 1, 3, 4 and 8 [18,31]. And, z-VAD-FMK could suppress the 2 major signaling pathways both with caspase 8 activation and with caspase 9 activation.

We previously reported a method for administering drugs into the inner ear of guinea pigs without causing damage [23,25], and this technique allows for the administration of drugs directly into the cochlea. There have been many reports describing the ototoxicity of aminoglycosides, including gentamicin [4,5,20]. Our method using the osmotic pump also could establish the animal model with the stable damage [24].

In this study, the administration of gentamicin caused malfunction of the inner ear and resulted in extensive cochlear hair cell death after 14 days. To test whether caspase inhibitors would protect against gentamicin ototoxicity, specific inhibitor agents were infused via osmotic pumps and exposed to cochlear tissues. In these experiments, we infused 250 μM of each caspase inhibitor solution at a rate of 0.5 μl/h. It was unclear what the final concentration of these agents was exposed to hair cells via the perilymph. But in a previous study from our laboratory, we infused neurotrophic factor into the cochlea of guinea pigs at a 10-fold molar excess of the levels used in the corresponding in vitro studies [13,21,26], and showed neurotrophic effects against intense sound exposure in the same animal model [25]. Therefore, we postulated that the about 10th concentration of inhibitor infused into the cochlea were exposed to cochlear tissues because of the dilution with perilymph. We used 250 μM concentrations of caspase inhibitors in the osmotic pumps, as these inhibitors have been shown to be effective at final concentrations of between 5 and 30 μM [1,9]. The caspase inhibitors used in our study were dissolved in a DMSO solution, as they are water-insoluble. And, further experiments using high concentrations of these inhibitor solutions could not be performed due to the appearance of DMSO cytotoxicity.

In the present study, the administrated caspase inhibitors could not protect all the hair cells. We administrated the caspase inhibitors in parallel with gentamicin. Meanwhile, Matsui et al. reported the perfectly protective effect of the inhibitors on the chick vestibular hair cells [17]. They started the infusion of the inhibitors 1 day before the insult with the aminoglycoside. If only inhibitors are administrated to the cochleae before insults, the stronger protective effects may appear. We thought that these are remaining problems and hope to perform the next experiments about this with taking the next opportunity.

The inhibition of caspases could thus prove to be a new prophylactic approach to the prevention of inner ear damage by aminoglycosides. For the treatment of inner ear diseases, drugs, such as steroids have been administered systemically but the permissible dosages are limited due to side effects.

Topical treatment of the inner ear has also been reported recently and has now been used in clinical practice [10,14]. Caspase inhibitors are, therefore, potential candidates for new agents, which may be administrated to the inner ear in topical treatments, but more in vivo experiments will be required in future to assess this possibility.

Acknowledgement

This study was supported by a scientific research grant from the Ministry of Education, Science, Sports, Culture and Technology of Japan (B (2) 14370544).

References

[1] Amel Kashipaz MR, Huggins ML, Powell RJ, Todd I. Human autologous mixed lymphocyte reaction as an in vitro model for autoreactivity to apoptotic antigens. Immunology 2002;107:358–65.
[2] Budihardjo I, Oliver H, Lutter M, Luo X, Wang X. Biochemical pathways of caspase activation during apoptosis. Annu Rev Cell Dev Biol 1999;15:269–90.
[3] Cheng AG, Huang T, Stracher A, Kim A, Liu W, Malgrange B, et al. Calpain inhibitors protect auditory sensory cells from hypoxia and neurotrophin-withdrawal induced apoptosis. Brain Res 1999;850: 234–43.
[4] Conlee JW, Gill SS, McCandless PT, Creel DJ. Differential susceptibility to gentamicin ototoxicity between albino and pigmented guinea pigs. Hear Res 1989;41:43–51.
[5] Conlon BJ, Smith DW. Topical aminoglycoside ototoxicity: attempting to protect the cochlea. Acta Otolaryngol 2000;120:596–9.
[6] Cunningham LL, Cheng AG, Rubel EW. Caspase activation in hair cells of the mouse utricle exposed to neomycin. J Neurosci 2002;22:8532–40.
[7] Forge A. Outer hair cell loss and supporting cell expansion following chronic gentamicin treatment. Hear Res 1985;19:171–82.
[8] Li L, Nevill G, Forge A. Two modes of hair cell loss from the vestibular sensory epithelia of the guinea pig inner ear. J Comp Neurol 1995;355:405–17.
[9] Grand RJ, Schmeiser K, Gordon EM, Zhang X, Gallimore PH, Turnell AS. Caspase-mediated cleavage of adenovirus early region 1A proteins. Virology 2002;301:255–71.
[10] Hoffer ME, Kopke RD, Weisskopf P, Gottshall K, Allen K, Wester D. Microdose gentamicin administration via the round window microcatheter: results in patients with Meniere's disease. Ann NY Acad Sci 2001;942:46–51.
[11] Hu BH, Henderson D, Nicotera TM. Involvement of apoptosis in progression of cochlear lesion following exposure to intense noise. Hear Res 2002;166:62–71.
[12] Hu BH, Henderson D, Nicotera TM. F-actin cleavage in apoptotic outer hair cells in chinchilla cochleas exposed to intense noise. Hear Res 2002;172:1–9.
[13] Kelpke SS, Reiff D, Prince CW, Thompson JA. Acidic fibroblast growth factor signaling inhibits peroxynitrite-induced death of osteoblasts and osteoblast precursors. J Bone Miner Res 2001;16: 1917–25.
[14] Lehner R, Brugger H, Maassen MM, Zenner HP. A totally implantable drug delivery system for local therapy of the middle and inner ear. Ear Nose Throat J 1997;76:567–70.
[15] Liu W, Staecker H, Stupak H, Malgrange B, Lefebvre P, VanDeWater TR. Caspase inhibitors prevent cisplatin-induced apoptosis of auditory sensory cells. Neuroreport 1998;9:2609–14.
[16] Matsui JI, Ogilvie JM, Warchol ME. Inhibition of caspases prevents ototoxic and ongoing hair cell death. J Neurosci 2002;22:1218–27.
[17] Matsui JI, Haque A, Huss D, Messana EP, Alosi JA, Roberson DW, et al. Caspase inhibitors promote vestibular hair cell survival and function after aminoglycoside treatment in vivo. J Neurosci 2003;23:6111–22.
[18] Muzio M, Chinnaiyan AM, Kischkel FC, O'Rourke K, Shevchenko A, Ni J, et al. FLICE, a novel FADD-homologous ICE/CED-3-like protease, is recruited to the CD95 (Fas/APO-1) death-inducing signaling complex. Cell 1996;85:817–27.
[19] Nakagawa T, Yamane H, Shibata S, Takayama M, Sunami K, Nakai Y. Two modes of auditory hair cell loss following acoustic overstimulation in the avian inner ear. ORL J Otorhinolaryngol Relat Spec 1997;59:303–10.
[20] Polgar R, Collison T, Slepecky NB, Wanamaker HH. Anatomic and morphometric changes to gerbil posterior cristas following transtympanic administration of gentamicin and streptomycin. J Assoc Res Otolaryngol 2001;2:147–58.
[21] Reiff DA, Kelpke S, Rue 3rd L, Thompson JA. Acidic fibroblast growth factor attenuates the cytotoxic effects of peroxynitrite in primary human osteoblast precursors. J Trauma 2001;50:433–9.
[22] Samejima K, Tone S, Kottke TJ, Enari M, Sakahira H, Cooke CA, et al. Transition from caspase-dependent to caspase-independent mechanisms at the onset of apoptotic execution. J Cell Biol 1998;143:225–39.
[23] Shimogori H, Yamashita H, Watanabe T, Nakamura S. A role of glucocorticoid receptors in the guinea pig vestibular system. Brain Res 1999;851:258–60.
[24] Shimogori H, Yamashita H. Effectiveness and utility of chemical labyrinthectomy with streptomycin using osmotic pump. ORL J Otorhinolaryngol Relat Spec 2000;62:60–2.
[25] Sugahara K, Shimogori H, Yamashita H. The role of acidic fibroblast growth factor in recovery of acoustic trauma. Neuroreport 2001;12: 3299–302.
[26] Thorns V, Licastro F, Masliah E. Locally reduced levels of acidic FGF lead to decreased expression of 28-kda calbindin and contribute to the selective vulnerability of the neurons in the entorhinal cortex in Alzheimer's disease. Neuropathology 2001;21:203–11.
[27] Ueda S, Masutani H, Nakamura H, Tanaka T, Ueno M, Yodoi J. Redox control of cell death. Antioxid Redox Signal 2002;4:405–14.
[28] Wersall J. Ototoxic antibiotics: a review. Acta Otolaryngol Suppl 1995;519:26–9.
[29] Wu WJ, Sha SH, Schacht J. Recent advances in understanding aminoglycoside ototoxicity and its prevention. Audiol Neurootol 2002;7:171–4.
[30] Xiang J, Chao DT, Korsmeyer SJ. BAX-induced cell death may not require interleukin 1 beta-converting enzyme-like proteases. Proc Natl Acad Sci USA 1996;93:14559–63.
[31] Yang B, El Nahas AM, Fisher M, Wagner B, Huang L, Storie I, et al. Inhibitors directed towards caspase-1 and -3 are less effective than pan caspase inhibition in preventing renal proximal tubular cell apoptosis. Nephron Exp Nephrol 2004;96:39–51.

Available online at www.sciencedirect.com
SCIENCE DIRECT
ELSEVIER
European Journal of Pharmacology 522 (2005) 116–121
ejp
www.elsevier.com/locate/ejphar

Post-exposure administration of edaravone attenuates noise-induced hearing loss

Kuniyoshi Tanaka, Tsuyoshi Takemoto, Kazuma Sugahara, Takeshi Okuda, Takefumi Mikuriya, Kenji Takeno, Makoto Hashimoto, Hiroaki Shimogori, Hiroshi Yamashita *

Department of Otolaryngology, Yamaguchi University School of Medicine, Minamikogushi 1-1-1, Ube, Yamaguchi 755-8505, Japan

Received 11 April 2005; received in revised form 8 August 2005; accepted 15 August 2005
Available online 3 October 2005

Abstract

We investigated the effects of the antioxidant edaravone against acoustic trauma in guinea pigs. Edaravone (1.722×10^{-2} M) was infused into the right ear by an osmotic pump, and the left ear was untreated for control. Animals received edaravone 9 h before (−9 h group, $n=7$) and 9 h (+9 h group, $n=8$), 21 h (+21 h group, $n=7$) and 33 h (+33 h group, $n=4$) after 3-h exposure to 130-dB noise. Seven days after noise exposure, we examined the shift in auditory brainstem response thresholds and histopathologic characteristics of the sensory epithelia. The smallest shift in auditory brainstem response threshold and smallest proportion of missing outer hair cells were observed in the +9 h group. This result was supported by immunohistochemical analysis of 4-hydroxy-2-nonenal. Our data suggest that edaravone may be clinically effective in the treatment of acoustic trauma, especially if given within 21 h of noise exposure.

Keywords: Edaravone; Cochlear protection; Antioxidant; Reactive oxygen species; Acoustic trauma; 4-HNE(4-hydroxy-2-nonenal)

1. Introduction

Noise exposure leads to increased levels of reactive oxygen species in the cochlea (Yamane et al., 1995), and noise-induced hearing loss can be reduced by treatment with antioxidants (Yamasoba et al., 1999; Kopke et al., 2000; Ohinata et al., 2000, 2003; McFadden et al., 2001; Lynch et al., 2004). However, these drugs have not been used in clinical settings.

Edaravone (3-methyl-1-phenyl-2-pyrazolin-5-1) is the first free-radical scavenger used in clinical practice in Japan, where it is used to treat acute cerebral infarction (Yamamoto et al., 1997). There are some studies showing an effect of edaravone on the inner ear (Horiike et al., 2003, 2004; Maetani et al., 2003; Takemoto et al., 2004). Takemoto et al. (2004) reported that pre-exposure perilymphatic application of edaravone reduced noise-induced hearing loss in guinea pigs. Thus, in the present study, we administered edaravone to guinea pigs before and after noise exposure, and investigated the optimal timing for administration of edaravone to protect the cochlea. In addition, at various time points after noise exposure we measured levels of 4-hydroxy-2-nonenal (4-HNE), which is a phospholipid peroxidation product generated by the reaction of free radicals with the plasma membrane.

2. Materials and methods

2.1. Animals

We used 34 male Hartley guinea pigs (300–450 g each; Chiyoda, Tokyo, Japan) with normal Preyer's reflexes and normal tympanic membranes. Twenty-six animals were divided into four treatment groups as described below, and 8 animals were used for immunohistochemical analysis of 4-HNE, also described below. This experiment was reviewed by the Committee for the Ethics of Animal Experiments in Yamaguchi University School of Medicine and carried out according to the Guideline for Animal Experiments of Yamaguchi University School of Medicine and The Law (No. 105) and Notification No. 6 of the Japanese Government.

* Corresponding author. Tel./fax: +81 836 22 2280.
E-mail address: hiro-shi@yamaguchi-u.ac.jp (H. Yamashita).

0014-2999/$ - see front matter © 2005 Elsevier B.V. All rights reserved.
doi:10.1016/j.ejphar.2005.08.026

2.2. Pump implantation

An osmotic pump (Model 2002, Alza Co., Palo Alto, CA, USA) filled with saline was implanted in the right ear of 26 guinea pigs, and the left ear was kept intact as a control. The pigs were anesthetized with a mixture of ketamine (16 mg/kg, i.p.) and xylazine (16 mg/kg, i.p.). After hypodermic injection of 1.5 ml 1% lidocaine, the temporal bone was exposed via postauricular incision. The mastoid bulla was opened with a 4-mm diamond burr to allow visualization of the round window. A tiny hole was made with a needle at a distance of 1 mm from the round window. The tip of the catheter was inserted into the hole, and saline was infused into the perilymphatic space of the cochlea. The polyethylene catheter was fixed to the mastoid bulla with dental cement (GC Fuji I, GC Co., Tokyo, Japan). The skin incision was closed and treated with antibiotic. The flow rate of the pump was 0.5 l/h. The osmotic pump was connected to a 10-cm polyethylene catheter (inner diameter=0.28 mm, outer diameter=0.61 mm; Becton Dickinson, Franklin Lakes, NJ, USA) and a 1-mm Teflon catheter (inner diameter=0.18 mm, outer diameter=0.3 mm; Unique Medical, Tokyo, Japan). The pump and catheter were filled with saline.

2.3. Pump exchange

The implanted osmotic pump was replaced by another pump filled with 1.722×10^{-2} M edaravone (Mitsubishi Pharma Co., Osaka, Japan), the concentration used in a previous in vivo study (Yamamoto et al., 1997). Edaravone was dissolved in 1 mol/l NaOH and water just prior to use, and the pH was adjusted to 7 with 1 mol/l HCl. The pumps were replaced under xylazine and ketamine general anesthesia. After hypodermic injection of 1.5 ml 1% lidocaine, an incision was made on each animal's back, and the saline-filled osmotic pump was replaced by an edaravone-filled pump. After the incision was closed, antibiotic ointment was applied to the incision site. The catheter was designed to begin administration of edaravone to the cochlear perilymph 12 h after pump exchange. In one group of animals, pumps were changed 21 h before noise exposure, and edaravone administration was started 9 h before noise exposure (−9 h group, $n=7$). In another group, pumps were changed immediately before noise exposure, and edaravone administration was started 9 h after noise exposure (+9 h group, $n=8$). In a third group and a fourth group, pumps were changed 9 and 21 h, respectively, after noise exposure, and edaravone administration was started 21 and 33 h, respectively, after noise exposure (+21 h group, $n=7$, and +33 h group, $n=4$, respectively).

2.4. Noise exposure

Guinea pigs under pentobarbital anesthesia (33 mg/kg, i.p.) were exposed to intense (130 dB sound pressure level) band noise centered at 4 kHz for 3 h. The noise we used was designed to cause permanent threshold shifts and to damage cochlear hair cells at the basal end of the second turn (Yamasoba et al., 1999). Each animal was immobilized, and a speaker was centered over the animal's head at a distance of 15 cm. The sound intensity was monitored with a sound-level meter (NA-60, Rion, Tokyo, Japan) positioned near the external auditory canal.

2.5. Auditory brainstem responses

The auditory brainstem response threshold was examined in guinea pigs under xylazine (16 mg/kg, i.p.) and ketamine (16 mg/kg, i.p.) anesthesia 3 days after pump implantation and 7 days after noise exposure. Responses were recorded between subcutaneous stainless steel electrodes located at the vertex (positive) and antinion (negative); the lower back served as the ground. The sound stimuli consisted of 2-, 4-and 8-kHz tone bursts (rise–fall time 2 ms, duration 4 ms). Stimuli were presented through a 10-cm-long tube that connected an earphone to the external auditory canal. The stimulus intensity was evaluated with a NA-60 sound-level meter adjacent to the tip of the tube. Responses to 500 stimuli were recorded with a signal processor (Synax 1100, NEC Co., Tokyo, Japan). The auditory brainstem response threshold was defined as the lowest stimulus intensity that produced a reliable waveform of 3–5 peaks.

2.6. Histopathology

One week after noise exposure, auditory brainstem response thresholds were recorded, and the 26 guinea pigs were killed with an overdose of pentobarbital. Both temporal bones of each animal were removed. The cochlea was opened at the apex, base and oval window and perfused with fixative (4% paraformaldehyde in 0.01 M phosphate-buffered saline (PBS), pH 7.3) gently for 12 h. The cochlea was rinsed in PBS, and the organ of Corti in the second turn of the cochlea was removed. The specimen was permeabilized with 0.3% Triton X-100 (Katayama Chemical Inc., Osaka, Japan) for 10 min and subsequently incubated with fluorescein isothiocyanate-conjugated phalloidin (1:50 dilution; Sigma, St. Louis, MO, USA) at room temperature for 1 h. The specimen was rinsed in PBS and then mounted using a SlowFade Light Antifade Kit (Molecular Probes, Eugene, OR, USA). The surface structure of each specimen was observed under a fluorescence microscope (Zeiss, Jena, Germany). The missing inner hair cells and outer hair cells in the second turn of the cochlea were counted, and the percentage of missing outer hair cells was recorded.

2.7. Immunohistochemistry for 4-HNE

We examined 4-HNE production in animals that did not receive edaravone. Animals were exposed to the same experimental noise conditions and killed at three different time points (immediately, 9, and 21 h) after noise exposure ($n=2$ each group). Two animals that were unexposed served as controls ($n=2$). The temporal bones were removed under deep pentobarbital anesthesia and transferred to 4% paraformaldehyde as described above and kept in fixative overnight. The tissue was decalcified in 5% ethylene diamine tetraacetic acid (pH 7.2) for approximately 14 days. The lateral walls of the cochleae were removed with a micromanipulator.

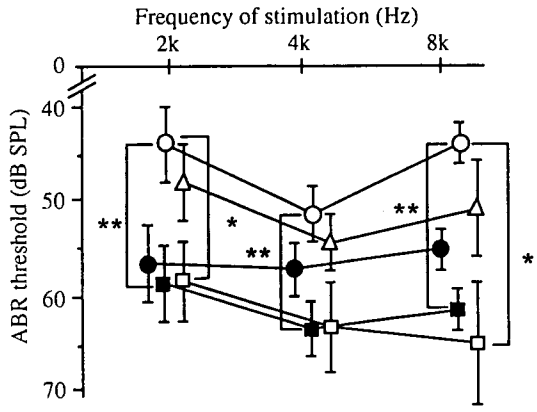

Fig. 1. Auditory brainstem response thresholds of edaravone-treated ears in the −9h group (closed circles), +9 h group (open circles), +21 h group (open triangles) and +33 h group (open squares) and control ears in all groups (closed squares) 1 week after noise exposure. The smallest auditory brainstem response threshold shifts were seen in the treated ears in the +9 h group. Error bar± 1 S.E.M., $^{**}P<0.01$, $^{*}P<0.05$.

Specimens were rinsed in PBS, incubated in methanol for 20 min at −20 °C, and then hydrated in PBS containing 0.1% Triton X-100 for 10 min. Specimens were soaked in PBS/2% dried milk for 2 h at 4 °C and then incubated for 12 h at 4 °C in a 1 : 100 dilution of anti-4-HNE mouse monoclonal antibody (OXIS International, Inc., Portland, OR, USA). The specimens were rinsed in PBS and incubated for 8 h at 4 °C in a 1 : 100 dilution of Alexa Fluor® 568-conjugated goat anti-mouse IgG (Molecular Probes). They were then rinsed in PBS and embedded in a semi-water-soluble resin (Immuno-Bed®, Polysciences, Inc., Washington, DC, USA) and cut into 2-μm-thick sections. Sections were counterstained with 4′ 6-diamino-2-phenylindole (DAPI) (Vectashield®, Vector Laboratories, Inc., Burlingame, CA, USA). Immunolabeling was visualized under brightfield illumination by means of a fluorescence microscope with a 20× objective.

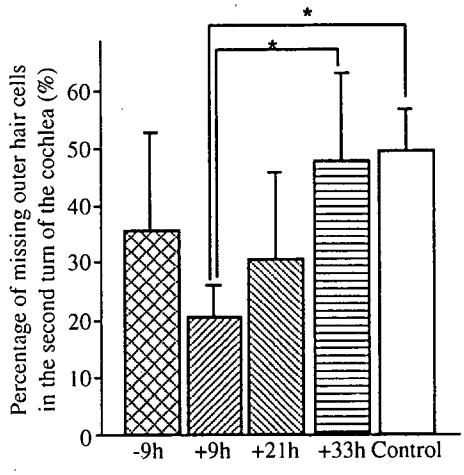

Fig. 2. Percentage of missing outer hair cells in the second turn of the cochlea 1 week after noise exposure. The number of missing outer hair cells was lower in the edaravone-treated ears than in the control ears in the −9, +9 and +21 h groups. In the +33 h group, there was no significant difference between edaravone-treated and control ears. Error bar± 1 S.E.M., $^{*}P<0.05$.

2.8. Statistical analysis

The differences in post-exposure auditory brainstem response thresholds and percentages of missing outer hair cells among the four groups and between treated and untreated ears were analyzed by Mann–Whitney *U*-test with StatView version 4.5J for Macintosh (Abacus Concepts, Berkley, CA, USA). *P* values less than 0.05 were accepted as statistically significant.

3. Results

3.1. Auditory brainstem response thresholds

There was no difference between the auditory brainstem response thresholds of treated and control ears before noise exposure (data not shown). Implantation of the osmotic pump and intracochlear infusion of saline had little influence on the auditory brainstem response threshold. In all animals, the

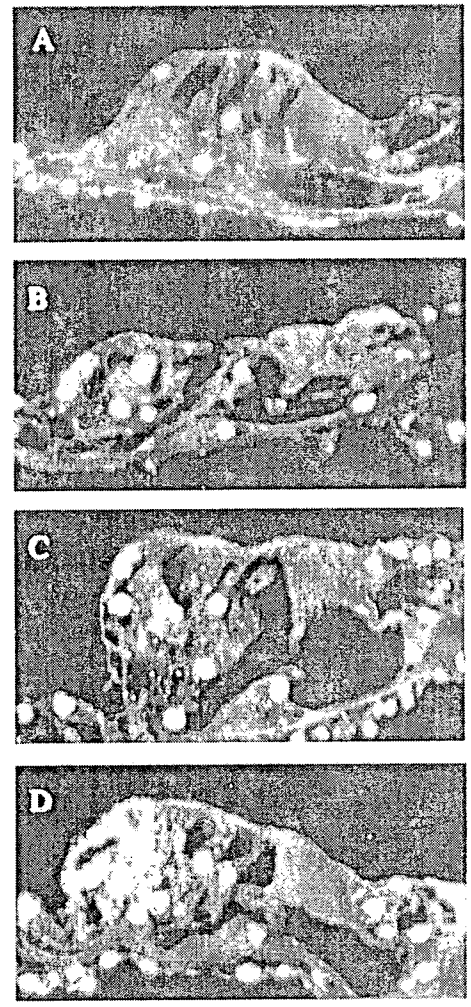

Fig. 3. Immunoreactivity to 4-hydroxy-2-nonenal (4-HNE) (red) in the organ of Corti following noise exposure. Nuclei were visualized with DAPI counterstaining (blue). Sections were taken from an area of the main lesion of the second turn of the cochlea. (A) Control; (B) immediately after noise exposure; (C) 9 h after noise exposure; (D) 21 h after noise exposure. (For interpretation of the references to colour in this figure legend, the reader is referred to the web version of this article.)

auditory brainstem response thresholds of both ears were increased 7 days after noise exposure (Fig. 1). However, the threshold shift was smaller in the treated ears than in the control ears, in the −9, +9 and +21 h groups. In the +33 h group, there was little difference between the thresholds of the treated and control ears. Of the treated ears, the threshold shift was the smallest in the +9 h group.

3.2. Outer hair cell counts

After noise exposure, all animals showed a loss of outer hair cells in the second turn of the cochlea. The inner hair cells of all ears were relatively well preserved (data not shown). In the −9, +9 and +21 h groups, the percentage of missing outer hair cells was lower in the edaravone-treated ears than in the control ears, but in the +33 h group, there was no significant difference between the treated and control ears (Fig. 2). The smallest percentage of lost hair cells was observed in the edaravone-treated ears in the +9 h group.

3.3. Immunohistochemistry for 4-HNE

All sections for 4-HNE assessment were taken from the main lesion of the second turn (approximately 9–12 mm from the apex). Staining was absent from negative control material tested without the primary antibody (not shown). Slight staining was observed in the organ of Corti and the stria vascularis of unexposed control animals (Figs. 3A, 4A). Organ of Corti sections from animals killed immediately after noise exposure (Fig. 3B) showed little immunoreactivity. However, sections from animals killed 9 h after noise exposure (Fig. 3C) showed immunoreactivity against 4-HNE in some cells of the organ of Corti. Increased HNE staining was seen in the region of the Hensen cells and Claudius cells 21 h after noise exposure (Fig. 3D). Stria vascularis sections from animals killed immediately after noise exposure (Fig. 4B) showed 4-HNE immunoreactivity, and the extent of specific immunoreactivity increased with time (Fig. 4C, D). In the spiral ganglion, 4-HNE immunoreactivity at each time point did not differ significantly from that of controls (not shown).

4. Discussion

In the present study, edaravone did not provide sufficient cochlear protection in the −9 h group, which received edaravone starting 9 h before noise exposure; however, less cochlear damage was observed in the +9 and +21 h groups, which received edaravone beginning 9 and 21 h, respectively, after noise exposure. One reason for this discrepancy may be the stability of edaravone in the pumps. The pharmacological action of edaravone gradually decreases after edaravone is dissolved in saline; however, its efficacy is reported to be stable up to 24 h after edaravone is dissolved (Mitsubishi Pharma Co.; personal communication). If edaravone is effective 24 h after it is dissolved, edaravone administered between 12 and 24 h after pump exchange should be effective. In the −9 h group, edaravone was administered until the end of noise exposure. In the +9, +21 and +33 h groups, edaravone was administered until 21, 33 and 45 h, respectively, after noise exposure. It is also possible that most free radical formation occurred several hours after noise exposure. Immunohistochemical analysis of the organ of Corti revealed that 4-HNE did not form immediately after noise exposure. 4-HNE was first detected 9 h after noise exposure and staining was increased 21 h after noise exposure. Yamashita et al. (2004) also reported the delayed formation of 4-HNE in the organ of Corti

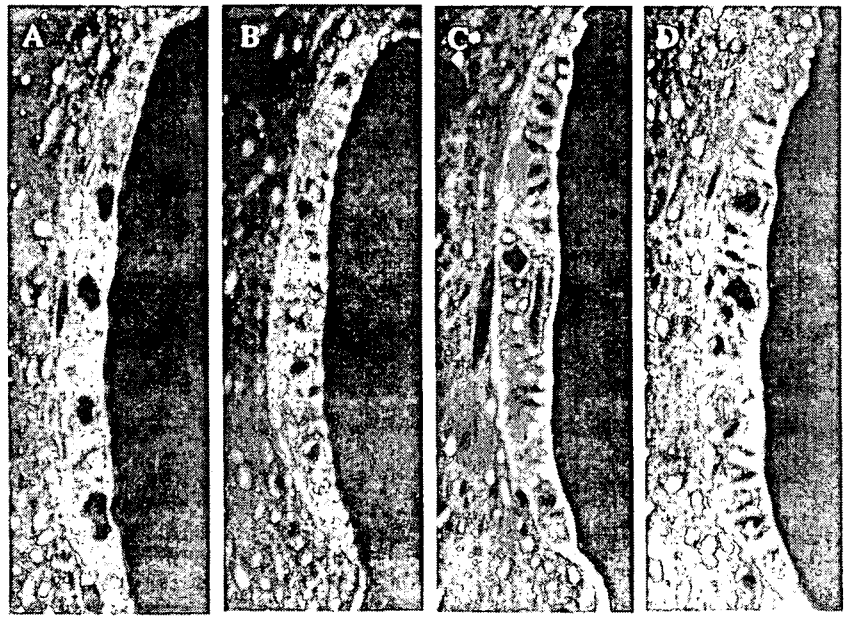

Fig. 4. Immunoreactivity to 4-HNE (red) in the stria vascularis following noise exposure. Nuclei were visualized with DAPI counterstaining (blue). Sections were taken from the main lesion of the second turn of the cochlea. (A) Control; (B) immediately after noise exposure; (C) 9 h after noise exposure; (D) 21 h after noise exposure. (For interpretation of the references to colour in this figure legend, the reader is referred to the web version of this article.)

following noise exposure. Therefore, we speculate that the main damage in the organ of Corti occurs between 9 and 21 h after noise exposure. Edaravone-treated ears of the +9 h group showed the least damage.

The causes of noise-induced hearing loss remain unclear. One of the many mechanisms by which sound may damage the cochlea is through cochlear ischemia and reperfusion injury. Reduced cochlear blood flow and/or intracochlear oxygen levels (Thorne and Nuttall, 1987; Lamm and Arnold, 1998, 2000; Miller et al., 2003) and vasoconstriction of cochlear capillaries (Hawkins, 1971) in response to noise have been reported. These findings suggest that ischemia and subsequent reperfusion are important pathophysiological processes in noise-induced hearing loss. Reperfusion is known to cause extensive tissue injury. Kaminski et al. (2002) reported that reactive oxygen species and neutrophils interact with each other and are the key players in reperfusion injury. Activated neutrophils migrate from the vascular compartment to ischemic tissue and are one of the main sources of reactive oxygen species during reperfusion. In this study, 4-HNE was first detected in the organ of Corti, followed by the stria vascularis. During ischemia, neutrophils remained and reactive oxygen species were generated in the lumen of the stria vascularis because of vasoconstriction of cochlear capillaries. After the restoration of blood flow, however, neutrophils migrated from the stria vascularis to ischemic tissue, such as the organ of Corti, and reactive oxygen species were generated in the organ of Corti. Lamm and Arnold (1998, 2000) showed that cochlear blood flow and perilymphatic oxygen tension declined gradually during 30 min of noise exposure and for 180 min thereafter. Therefore, it is thought that ischemia was prolonged and the start of reperfusion was delayed, although noise did not cause complete ischemia. Additionally, Albertine et al. (1994) showed that ischemia-reperfusion causes a three-fold increase in neutrophil numbers in the lumen of arterioles and venules by 60 min of reperfusion and up to a seven-fold increase by 270 min of reperfusion. In this study, 4-HNE staining was observed in the supporting cells, not the outer hair cells, within 21 h, and it seems that the immunostaining spreads to the outer hair cells 21 h later. Yamashita et al. (2004) reported that immunostaining had spread to all cells of the organ of Corti at 7 days after the noise exposure. These reports and our results demonstrate that post-exposure administration of edaravone is important because the events that lead to the generation of reactive oxygen species, such as reperfusion and infiltration by neutrophils, occur well after noise exposure.

Our osmotic pump method (Sugahara et al., 2001) allows continuous microinjection into the inner ear, so the effect of edaravone is enhanced. Several drug-delivering systems are used clinically. One method of delivery is to place edaravone-soaked Gelfoam on the round window; this does not damage the cochlea (Horiike et al., 2003, 2004). Intratympanic drug injection is also a possible means of drug delivery (Doyle et al., 2004).

We conclude that topical administration of edaravone may prevent noise-induced hearing loss and that edaravone treatment will be clinically effective, especially if given within 21 h of noise exposure.

Acknowledgments

This work was supported by a grant from the Japanese Ministry of Education, Culture, Sports, Science and Technology.

References

Albertine, K.H., Weyrich, A.S., Ma, X.L., Lefer, D.J., Becker, L.C., Lefer, A.M., 1994. Quantification of neutrophil migration following myocardial ischemia and reperfusion in cats and dogs. J. Leukoc. Biol. 55, 557–566.

Doyle, K.J., Bauch, C., Battista, R., Beatty, C., Hughes, G.B., Mason, J., Maw, J., Musiek, F.L., 2004. Intratympanic steroid treatment: a review. Otol. Neurotol. 25, 1034–1039.

Hawkins Jr., J.E., 1971. The role of vasoconstriction in noise-induced hearing loss. Ann. Otol. Rhinol. Laryngol. 80, 903–913.

Horiike, O., Shimogori, H., Ikeda, T., Yamashita, H., 2003. Protective effect of edaravone against streptomycin-induced vestibulotoxicity in the guinea pig. Eur. J. Pharmacol. 464, 75–78.

Horiike, O., Shimogori, H., Yamashita, H., 2004. Effect of edaravone on streptomycin-induced vestibulotoxicity in the guinea pig. Laryngoscope 114, 1630–1632.

Kaminski, K.A., Bonda, T.A., Korecki, J., Musial, W.J., 2002. Oxidative stress and neutrophil activation—the two keystones of ischemia/reperfusion injury. Int. J. Cardiol. 86, 41–59 (Review).

Kopke, R.D., Weisskopf, P.A., Boone, J.L., Jackson, R.L., Wester, D.C., Hoffer, M.E., Lambert, D.C., Charon, C.C., Ding, D.L., McBride, D., 2000. Reduction of noise-induced hearing loss using L-NAC and salicylate in the chinchilla. Hear. Res. 149, 138–146.

Lamm, K., Arnold, W., 1998. The effect of prednisolone and non-steroidal anti-inflammatory agents on the normal and noise-damaged guinea pig inner ear. Hear. Res. 115, 149–161.

Lamm, K., Arnold, W., 2000. The effect of blood flow promoting drugs on cochlear blood flow, perilymphatic pO_2 and auditory function in the normal and noise-damaged hypoxic and ischemic guinea pig inner ear. Hear. Res. 141, 199–219.

Lynch, E.D., Gu, R., Pierce, C., Kil, J., 2004. Ebselen-mediated protection from single and repeated noise exposure in rat. Laryngoscope 114, 333–337.

Maetani, T., Hakuba, N., Taniguchi, M., Hyodo, J., Shimizu, Y., Gyo, K., 2003. Free radical scavenger protects against inner hair cell loss after cochlear ischemia. NeuroReport 14, 1881–1884.

McFadden, S.L., Ohlemiller, K.K., Ding, D., Shero, M., Salvi, R.J., 2001. The influence of superoxide dismutase and glutathione peroxidase deficiencies on noise-induced hearing loss in mice. Noise Health 3, 49–64.

Miller, J.M., Brown, J.N., Schacht, J., 2003. 8-*iso*-prostaglandin F (2alpha), a product of noise exposure, reduces inner ear blood flow. Audiol. Neuro-Otol. 8, 207–221.

Ohinata, Y., Yamasoba, T., Schacht, J., Miller, J.M., 2000. Glutathione limits noise-induced hearing loss. Hear. Res. 146, 28–34.

Ohinata, Y., Miller, J.M., Schacht, J., 2003. Protection from noise-induced lipid peroxidation and hair cell loss in the cochlea. Brain Res. 966, 265–273.

Sugahara, K., Shimogori, H., Yamashita, H., 2001. The role of acidic fibroblast growth factor in recovery of acoustic trauma. NeuroReport 12, 3299–3302.

Takemoto, T., Sugahara, K., Okuda, T., Shimogori, H., Yamashita, H., 2004. The clinical free radical scavenger, edaravone, protects cochlear hair cells from acoustic trauma. Eur. J. Pharmacol. 487, 113–116.

Thorne, P.R., Nuttall, A.L., 1987. Laser Doppler measurements of cochlear blood flow during loud sound exposure in the guinea pig. Hear. Res. 27, 1–10.

Yamamoto, T., Yuki, S., Watanabe, T., Mitsuka, M., Saito, K., Kogure, K., 1997. Delayed neuronal death prevented by inhibition of increased hydroxyl radical formation in a transient cerebral ischemia. Brain Res. 762, 240–242.

Yamane, H., Nakai, Y., Takayama, M., Iguchi, H., Nakagawa, T., Kojima, A., 1995. Appearance of free radicals in the guinea pig inner ear after noise-induced acoustic trauma. Eur. Arch. Otorhinolaryngol. 252, 504–508.

Yamashita, D., Jiang, H.Y., Schacht, J., Miller, J.M., 2004. Delayed production of free radicals following noise exposure. Brain Res. 1019, 201–209.

Yamasoba, T., Schacht, J., Shoji, F., Miller, J.M., 1999. Attenuation of cochlear damage from noise trauma by an iron chelator, a free radical scavenger and glial cell line-derived neurotrophic factor in vivo. Brain Res. 815, 317–325.

ORL

ORL 2005;67:259–265
DOI: 10.1159/000089405

Published online: December 15, 2005

CGRP Expression in the Vestibular Periphery after Transient Blockage of Bilateral Vestibular Input

Hirotaka Hara Kenji Takeno Hiroaki Shimogori Hiroshi Yamashita

Department of Otolaryngology, Yamaguchi University School of Medicine, Ube, Yamaguchi, Japan

Key Words
Tetrodotoxin · Vestibular function · Osmotic pump · Calcitonin gene-related peptide

Abstract
This study aimed to establish an animal model of reversible bilateral vestibular disorders that is suitable for examining the mechanisms of vestibular plasticity, and to observe the changes in the plasticity of vestibular efferent systems. Tetrodotoxin (TTX) was infused continuously for 7 days into the bilateral perilymph of guinea pig cochlea. We assessed the vestibulo-ocular reflex (VOR) for evaluating the vestibular function. We also investigated the changes in calcitonin gene-related peptide (CGRP) immunoreactivity in vestibular end organs to observe the changes in the plasticity of vestibular systems. The VOR was completely eliminated by TTX administration and returned to the preoperative levels within 120 h after TTX discontinuation. An obvious increase in the number of CGRP-immunoreactive fibers was observed within the neurosensory epithelia of the maculae and cristae. An animal model of reversible bilateral vestibular disorders was established and used for investigating the plasticity of the vestibular nervous system.

Introduction

Patients with chronic bilateral vestibular deficits suffer from severe disequilibrium and exhibit instability while walking in the dark as a long-term sequela; neither of these is observed in patients with unilateral disorders. Recent studies also suggest that the complete loss of vestibular function may result in behavioral effects that are not observed in unilateral damage, for example, bilateral vestibular deficits may be a distinct cause of impairments in exploration and object recognition [1].

The management strategy for vestibulopathic patients includes the facilitation of vestibular compensation and habituation. However, for patients with bilateral vestibular deficits, management strategies, including hair cell regeneration and cell therapy, are expected to be developed in the near future.

It is important to investigate the mechanisms of central nervous system plasticity that are related to the resumption of vestibular input following long-term vestibular deficits. However, there have been few reports related to the plasticity of the central nervous system following reversible bilateral vestibular impairment [2, 3]. A majority of the experimental models that have been used so far to study the vestibular disorders were constructed by ablation or mechanical destruction of whole or partial vestibular end organs. However, the use of an-

KARGER
Fax +41 61 306 12 34
E-Mail karger@karger.ch
www.karger.com

0301–1569/05/0675–0259$22.00/0

Accessible online at:
www.karger.com/orl

Hirotaka Hara, MD
Department of Otolaryngology
Yamaguchi University School of Medicine
Ube, Yamaguchi 755-8505 (Japan)
Tel./Fax +81 836 22 2280, E-Mail harahiro@yamaguchi-u.ac.jp

imal models with surgical deafferentation of vestibular input is not suitable for investigating the mechanisms of vestibular plasticity that underlie reversible vestibular disorders.

It has been demonstrated that nerve conduction can be blocked by tetrodotoxin (TTX), the active element in puffer fish poison, without affecting the resting membrane potential [4]. Low TTX concentrations reversibly block nerve excitation by specifically inhibiting the increase in voltage-dependent sodium conductance of the nerve membrane [5]. This property has made TTX a commonly used drug for inhibiting nerve activity without permanently compromising the subject's anatomy.

Katsuki et al. [6], Pasic and Rubel [7], and Born and Rubel [8] have established that TTX, which is present in the perilymph of mammals and birds, reversibly blocks the activity of the auditory component of the VIIIth cranial nerve. Similarly, Weisleder and Rubel [9] reported reversible blockage of vestibular input in the vestibular nervous system on administration of an intralabyrinthine injection of TTX. Saxon [2, 11], Saxon and White [3], and Saxon et al. [10] also reported reversible blockage of vestibular input following transtympanic administration of TTX. These reports show that TTX can block vestibular input without the ablation of vestibular end organs.

The purpose of this study was to establish an animal model of reversible bilateral vestibular disorders that is suitable for examining the mechanisms of vestibular plasticity through continuous bilateral intracochlear administration of TTX by using an osmotic pump, and to observe changes in the plasticity of vestibular efferent systems.

We investigated the changes in calcitonin gene-related peptide (CGRP) immunoreactivity in the efferent system of the vestibular end organs when vestibular inputs were resumed after a 1-week absence. In adult mammals, the ampullar and macular vestibular receptors are extensively innervated by the efferent nerve fibers, but this highly branched network originates from a very small neuron population in the brainstem [12–14]. The fibers run principally through the basal part of the epithelium and form synapses either directly with type II sensory cells and the afferent nerve chalices that innervate type I sensory cells or contact the afferent nerve fiber endings on type II sensory cells. The organization of the efferent innervation network in the vestibular periphery has been described by the presence of one of its neurotransmitters or neuromodulators, the neuroactive peptide CGRP. Studies using immunoelectron microscopy [15] and confocal laser scanning microscopy [16] in which CGRP was used as a specific and exclusive efferent marker have demonstrated the extreme complexity and richness of these efferent preterminal fibers and axon terminals in rat sensory epithelium [17]. Therefore, in this study, we dealt with CGRP expression in the vestibular end organs in order to evaluate their plasticity.

Materials and Methods

Animals

Six male Hartley guinea pigs (weighing approximately 600 g) with normal Preyer's reflexes and tympanic membranes were used in this study. The experimental protocol was reviewed by the Committee for Ethics on Animal Experiments at Yamaguchi University School of Medicine. All experiments were carried out in accordance with these guidelines as well as Japanese Federal Law No. 105 and Notification No. 6 of the Japanese Government.

Osmotic Pump Implantation

We used an Alzet miniosmotic pump (model 2002; Alza Co., Palo Alto, Calif., USA) with a flow rate of 0.5 μl/h. The pump was connected to a 10-cm polyethylene catheter (i.d. = 0.28 mm, o.d. = 0.61 mm). Both the pump and the catheter were filled with 0.01 μg/μl of TTX (Sigma Chemical Co., St. Louis, Mo., USA). Under pentobarbital anesthesia (28 mg/kg, i.p.) and local anesthesia (1.5 ml of 1% lidocaine HCl), the temporal bone was bilaterally exposed via a postauricular incision. The mastoid bulla was opened using a diamond burr to allow visualization of the round window, and a second small hole was made beside the main hole to insert the polyethylene catheter. A tiny hole was made with a perforating burr at a distance of 1 mm from the round window. The tip of the catheter was inserted into the hole beside the round window, and TTX was infused into the perilymphatic space of the cochlea. The polyethylene catheter was attached to the mastoid bulla with dental cement (GC Fuji, Tokyo, Japan). After washing the wound with saline, a small amount of piperacillin sodium was introduced to prevent infection. Following wound closure, piperacillin sodium (40 mg/kg) was injected intramuscularly. The body temperature was maintained at 37°C during the operation and for 24 h postoperatively, and each animal was kept warm with an electric blanket.

Four animals were treated with 0.01 μg/μl of TTX solution (Sigma Chemical Co.). In our previous study, vestibular function was found to be within the preoperative range after implantation of the osmotic pump and infusion of saline [18, 19]; the auditory function was also found to be within the preoperative range [20]. Two animals were treated with sterile saline and used as control animals.

Evaluation of Vestibular Function

We measured the horizontal vestibulo-ocular reflex (VOR) using our method as previously reported [21, 22]. Briefly, in order to immobilize the guinea pig, a cage designed to hold the animal still during experiments was mounted on top of a turntable apparatus (Daiichi Medical, Tokyo, Japan). The animal's head was fixed firmly, and the eye movements of the guinea pigs were videotaped (Hi8 format; Sony, Tokyo, Japan) in the dark with an infrared CCD

camera (Nagashima Medical, Tokyo, Japan). We stored the video images on a computer (Power Mac G4; Apple Computer, Calif., USA). Each image was converted into an image file with QuickTime 4.0 optional (Apple Computer). For automatic analysis of the guinea pig's eye movements, we created a macro that could be used with the National Institutes of Health (NIH) Image analysis software (http://rsb.info.nih.gov/nih-image/). We calculated slow phase velocities, found the maximum slow phase velocity, and calculated the horizontal VOR gain by dividing the maximum slow phase velocity by the peak angular velocity. We measured the VOR gains with sinusoidal rotations at 0.1 Hz and a peak angular velocity of 60°/s before, 24 h after, and on day 7 of pump placement. On day 7, TTX administration was discontinued by clamping the catheter, and the VOR gains were measured at 24, 72, and 120 h after discontinuation.

Histological Examination

After the physiological evaluation, each animal was deeply anesthetized with pentobarbital. Transperilymphatic perfusion through the cochlear hole was performed with 4% paraformaldehyde in 0.1 *M* phosphate buffer, followed by immediate decapitation of the animals. After the temporal bone was dissected, the vestibule and semicircular canals were excised and soaked in the same fixative for 1 h. The specimen was then decalcified in 10% ethylenediaminetetraacetic acid for 1 h, rinsed in 0.01 *M* phosphate-buffered saline, dehydrated in a series of ethanol steps, and embedded in a water-soluble resin (JB-4; Polysciences Inc., Warrington, Pa., USA). Next, 2-μm-thick sections were cut and stained with toluidine blue and paraphenylenediamine; they were then visualized by using the ×100 oil immersion objective of a microscope (Nikon Corp., Tokyo, Japan).

Immunohistological Examination

The JB-4-embedded samples of 2 μm thickness were cut and placed on poly-*L*-lysine-coated slides. The ABC method was performed as follows. The slides were treated with: (i) distilled H_2O for 15 min to allow hydration, (ii) 4% H_2O_2 for 30 min, (iii) 2% normal goat serum in 0.3% Triton X-100 phosphate-buffered saline for 30 min, (iv) polyclonal anti-CGRP serum (1:400; Amersham Co., Japan) overnight at 25°C, (v) biotinylated goat antirabbit IgG (Nichirei Co., Japan) for 4 h, (vi) streptavidin-horseradish peroxidase (Nichirei Co., Japan) for 2 h, (vii) 3-amino-9-ethylcarbazole for 30 min, and (viii) counterstained with hematoxylin. These sections were examined by using a light microscope (Nikon Corp., Tokyo, Japan).

Results

Evaluation of Vestibular Function

VOR Examination. Figure 1 shows the changes in VOR gain during TTX administration and after TTX discontinuation. VOR was eliminated at 24 h after TTX initiation. The absence of VOR was sustained throughout TTX administration, and VOR gain returned to the preoperative level within 120 h after TTX discontinuation.

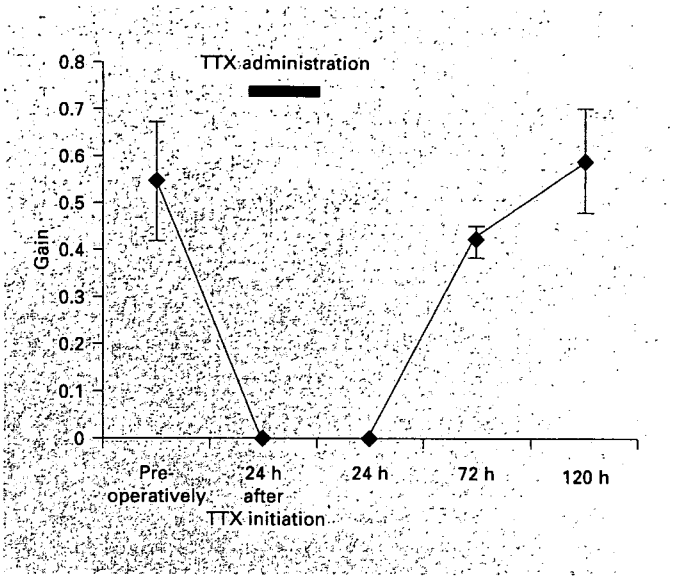

Fig. 1. VOR gains of experimental animals. VOR gain in TTX-treated animals was zero at 24 h after TTX administration and it recovered to pretreatment levels 120 h after TTX administration was discontinued. Error bar, ±1 SE.

Histological Examination: Labyrinth Morphology under Light Microscopy. Typical specimens at 7 days after TTX discontinuation did not show any obvious morphological changes in the sensory epithelial layer of the utricular macula (fig. 2) or in the cristae of the horizontal semicircular canal (fig. 3) when compared with the control animals.

Immunohistochemical Examination. A number of CGRP-immunoreactive fibers were observed in the utricular macula and ampullar cristae of the horizontal semicircular canals of the control guinea pigs. Many of these fibers were located in the connective tissue layer beneath the sensory epithelium (fig. 4A, B, fig. 5). On the other hand, the distribution of CGRP-immunoreactive fibers observed in the vestibular end organs of TTX-treated animals was different from that observed in the control animals. The CGRP-immunoreactive fibers were also located in the connective tissue layer beneath the sensory epithelium, but the number of CGRP-immunoreactive terminals within the neurosensory epithelia of the maculae and cristae was observed to have increased. These fibers appeared to leave the plexus and surround the sensory hair cells (fig. 6A, B, fig. 7).

Fig. 2. Light microscopic findings of the utricle. The otoconial layer was clearly observed. No degenerative changes in the hair cells were observed. Bar = 10 μm.

Fig. 3. Light microscopic findings of the horizontal crista ampullaris. No degenerative changes in hair cells were observed after continuous TTX administration. Bar = 10 μm.

Discussion

This study aimed to establish an animal model of reversible bilateral vestibular disorders that is suitable for examining the mechanisms of vestibular plasticity, and to observe changes in the plasticity of vestibular efferent systems. Using an osmotic pump to achieve continuous bilateral intracochlear administration of TTX, this study demonstrated that an animal model of transient vestibular disruption can be established without destroying the vestibular end organs.

TTX is a potent blocker of voltage-dependent sodium channels in excitable cells and has been successfully used in a number of studies on the auditory and vestibular nervous systems to produce a fully reversible blockage of action potentials [6–9]. Weisleder and Rubel [9] examined the changes in the vestibular function resulting from TTX administration by using vestibular-evoked potentials. They reported that a single dose (0.005 ml) of a 2.5×10^{-4}-mg TTX solution administered via bilateral oval windows resulted in the disappearance of vestibular-evoked potentials 30 min after the administration; the potentials returned to their baseline levels after 24 h [9]. Saxon et al. [10] reported that unilateral transtympanic administration of 3 m*M* TTX produced behavioral symptoms similar to those following unilateral peripheral vestibular ablation. They reported that the head tilt and neck torsion in the direction of TTX administration was evident between 30 and 60 min after TTX administration and that it persisted at varying degrees for >48 h. However, there have been no previous studies investigating the changes in vestibular function over time with continuous bilateral intracochlear administration of TTX. In addition to elucidating the central and peripheral vestibular plasticity induced by bilateral vestibular loss, this model may be useful for examining dizziness resulting from the loss of bilateral vestibular function.

Interestingly, when compared with previous studies in which TTX was administered once unilaterally [9–11], our data show that the recovery of vestibular functions was slow, although the TTX concentration administered during our study was lower than that in previous studies. There is increasing evidence that neuronal plasticity occurs within the peripheral and central pathways during and after space flight [23, 24]. Ross [24] described that a statistically significant increase in the total number of ribbon synapses and in sphere-like ribbons in both types of hair cells have been observed in adult rat utricles that were exposed to microgravity. Based on these studies, the adult mammalian vestibular end organs may retain the potential for synaptic plasticity [24]; the possible explanations for this finding include the possibility that continuous and bilateral blockage of vestibular inputs may result in extensive central and peripheral vestibular plasticity when the vestibular inputs resume.

The distribution of CGRP-immunoreactive fibers in the vestibular end organs of the control guinea pigs was similar to that reported previously [25–27].